Statistical Physics of Small Granular Systems with Hysteretic Interaction

Statistische Physik kleiner granularer Systeme mit hysteretischer Wechselwirkung

Von

Jan-Hendrik Trösemeier

aus

Stadtoldendorf

am Max-Planck-Institut für Dynamik und Selbstorganisation

an der Fakultät für Physik der Georg-August-Universität Göttingen

3. März 2012 bis 1. September 2012

Erstgutachter: **Apl. Prof. Jürgen Vollmer**
Zweitgutachter: **Apl. Prof. Ulrich Parlitz**

Abstract

We investigate the dynamics of hard disks with hysteretic and therefore dissipative interaction. Dissipation drives a system out of equilibrium naturally. In dilute systems the overall behavior is governed by two-particle interaction so that certain features of a granular system can already be analyzed for two hard-core particles with two-dimensional periodic boundary conditions. The description is analogue to a Sinai billiard. Augmenting this model with a hysteretic interaction makes it an ideal candidate for the study of simple out-of-equilibrium systems. Adding shear to the billiard allows us to inject energy to balance dissipation. Surprisingly, the absorbing state of a clustered system still persists even if the average energy increases. Up to now it was not clear which of those findings are specific features of the two-dimensional dynamical-system, and which carry over to many particles—and, if so, how this transfer should be done. To fill this gap we use Molecular Dynamics simulations for two and more particles to confirm the relevant findings on the two-particle system. The results are interpreted by comparison to pertinent dynamical-system results for small systems and to the predictions of kinetic theory for large systems. While doing this the assumptions of kinetic theory, in particular molecular chaos, are critically examined.

Acknowledgments

I would like to thank Prof. Jürgen Vollmer for his never-ending enthusiasm and motivation. I thank Prof. Parlitz for his commitment as a referee. Furthermore, I warmly thank Mitja Kleider, Johannes Blaschke, Artur Wachtel, Martin Rohloff, Bernhard Altanar, Izabella Benczik and Marco Mazza. Their input, motivation and the lively atmosphere were a constant source of motivation and inspiration.

Preface

Granulates are nearly-spherical agglomerates of matter that posses a large number of internal degrees of freedom [Radja and Roux, 2004]. These allow to dissipate energy on contact and thus are a good candidate for studies of non-equilibrium systems.
The natural length-scale of everyday granulates can be considered large enough to neglect further microscopic details [Puglisi, 2010]: For example, if we let the average distance between the grains become large enough the shape of the force-law with which they interact during impacts becomes unimportant because the duration of collisions becomes small in comparison to the average time between collisions. From this point of view grains behave like hard-spheres that reflect instantly on contact. The main difference to the well studied hard-sphere gas lies in the inelasticity of collisions [Zippelius, 2006]. Though the exact details behind dissipation are complicated [Aspelmeier, 2000], the main contributions are a loss of energy proportional to the relative velocity of the grains and a loss of a constant amount of energy. We will reference the former case as dry granulates and the latter as wet granulates.
The energy is dissipated into the microscopic degrees of freedom. Which of these mechanisms dominate depends on the length-scale and the material of the granulates [Luding, 2009] under consideration.
Even the simple model of only dissipating a fraction of relative velocity on contacts leads to a great many of phenomena in granular gases and there is extensive research performed in this area [Brilliantov and Pöschel, 2004; Nakagawa and Luding, 2009; Zippelius, 2006].
Of recent interest is augmenting the theory of dry granular matter to describe wet granular matter. Wet granulates are covered with a thin film of liquid. If two wet grains with a thin film collide, the surface tension of the film will lead to a liquid bridge between the grains that attracts the particles to one-another [Herminghaus, 2005; Mitarai and Nori, 2006]). Breaking the bridge costs a certain amount of energy. From the point of view of foundations of statistical physics such models are interesting because this is one of the simplest hysteretic interactions that dissipates energy on the microscopic level and thus breaks time reversal symmetry.
Following a larger system of grains interacting under this dynamics one observes that the system starts to form clusters since the average kinetic energy of the particles decreases due to the dissipative nature of hysteretic bridge ruptures [Fingerle, 2007; Röller, 2010]. To retain some sort of steady state, energy must be injected. Striving for a

model system that is simple, yet not artificial, one can think of shearing the system. This increases the system's energy and may lead to a non-equilibrium-steady-state where dissipation and shearing balance each other.
In order to understand this model system it is natural to follow the same route that kinetic theory takes [Reichl, 1980]: starting from the knowledge about two particle interaction one aims for a coarse-grained description of larger system. The route for achieving this up-scaling is well studied. However, it relies on certain assumptions, e.g., that the system is ergodic; and that correlations between disks decay sufficiently rapidly. Here we discuss how well these assumptions are fulfilled for small granular systems and how we can bridge the gap between two particle interaction to few-body systems.

Outline

In Chapter 2 we will provide an introduction into wet and dry granular matter and the connection to statistical physics. It turns out that dry granular matter provides a simple model with naturally hysteretic and therefore dissipative interaction. This in turn lends itself to study wet granulates in a non-equilibrium context. We also review the methods from kinetic theory of how to obtain a coarse grained description of a system whose fundamental pair interactions are known.

In Chapter 3 we discuss the statistical physics of small systems without dissipation. We estimate the collision frequency of a hard-sphere gas in the limit of few particles in a system with periodic boundary conditions. The periodic boundary conditions impose the conservation of the center of mass momentum which reduces the degrees of freedom of the gas. Hence we adjust, e.g., the Maxwellian energy distribution. In the limit of large number of particles we show that the classical limit is retained.

In Chapter 4 we study a wet system without energy injection in free cooling. We do this by using time driven Molecular Dynamics simulations that are compared to simulations of a Sinai billiard. For two disks both match nicely. We augment this by discussing the free cooling of three to ten disks. The main difference for more than two disks lies in that the one particle energy distribution has to be taken into account. Additionally, we confirm that the natural distribution is a uniform distribution conditioned by the system's energy. We also discuss the energy distribution in the limit of small energies, i.e., energies close to the bridge rupture energy.

In Chapter 5 shearing is introduced with Lees Edwards boundary conditions. This serves as an energy injection mechanism. We study the time dependence of the average energy and the ensemble energy distribution. It turns out that—although the average energy increases—the system still shows clustering. The reason can be found in the ensemble energy distribution.

Chapter 6 concludes the thesis and offers a perspective for future research.

Contents

Nomenclature

ϵ	Coefficient of restitution, relating initial - relative normal - velocity v_i^n to final velocity v_f^n via $\epsilon = v_f^n/v_i^n$, see equation (2.1), page 6
η	Grain viscosity, see equation (2.7), page 8
γ	Surface tension grain/liquid, see equation (2.10), page 9
$\hat{V}$	Liquid volume normalize with the volume of the grain it is wetting, see equation (2.12), page 10
$\{\mathcal{H}, \cdot\}$	Canonical Poisson bracket, see equation (1.4), page 5
$\mathcal{H}$	Hamiltonian, see equation (1.3), page 5
$\mathfrak{B}$	Bridge rupture operator, see equation (2.45), page 21
$\mathfrak{C}$	Collision operator, see equation (2.42), page 20
$\mathfrak{L}$	Lees Edwards boundary crossing operator, see equation (5.4), page 47
$\mathfrak{p}$	Periodic boundary crossing operator, see equation (2.48), page 21
ν	Poisson ratio, see equation (2.5), page 8
$\mathbf{x}_i$	Disk positions $\mathbf{x} \in \mathbb{R}$, see equation (2.3), page 7
θ	Direction of relative motion on the energy scale in the Sinai billiard, see equation (2.30), page 18
θ_c	Critical wetting angle, see equation (2.10), page 9
ξ	Overlap between two disks, see equation (2.3), page 7
A	Material constant for viscoelastic interaction, defined in [Brilliantov and Pöschel, 2001], see equation (2.6), page 8
C_i	Velocity auto correlation function, see equation (4.52), page 43
D	Diffusion constant in Shearing Chapter, see equation (5.11), page 48
D	Dimension, see equation (3.8), page 28
$d\Gamma$	Phase space volume, see equation (3.2), page 28
E	Kinetic Energy of Disks, see equation (2.2), page 6

E_{crit}	Critical center of mass energy, see equation (4.11), page 33
$f^{(N)}$	Reduced phase space density, see equation (1.5), page 5
F_{12}	Force between two disks, see equation (1.6), page 5
f_{coll}	Collision frequency, see equation (4.36), page 37
G	Center of mass position, see equation (3.10), page 29
I	Angular momentum of Sinai billiard, see equation (2.30), page 18
J	Jacobian, see equation (2.44), page 21
k	Boltzmann constant, see equation (3.8), page 28
M	Drift velocity, see equation (5.11), page 48
m_{eff}	Effective mass, see equation (3.15), page 30
N	Number of disks, see equation (3.8), page 28
p	Squared Energy of the Sinai billiard, see equation (2.30), page 18
p_L	Laplace pressure in toroidal liquid bridge, see equation (2.9), page 9
Q	Relative velocity projected on relative momentum. Normalized with the total momentum. Billiard coordinate., see equation (2.30), page 18
q	Relative billiard coordinates,$q_i = x_2 - x_1 = -\xi_i$., see equation (2.26), page 18
Q_{NVE}	Microcanonical Ensemble, see equation (3.1), page 27
R_1, R_2	Curvature of liquid film covering two grain with toroidal shape, see equation (2.9), page 9
r_i	Disk radius, see equation (2.3), page 7
R_{eff}	Effective radius of two disks, see equation (2.4), page 7
s_c	Bridge rupture distance, see equation (2.12), page 10
T	Granular temperature, $T \doteq \frac{2}{D}\frac{1}{N}\sum_{i=1}^{N}\frac{1}{2}m_i\mathbf{v}_i^2$., see equation (4.34), page 37
T	Temperature, see equation (3.8), page 28
Y	Young's modulus, see equation (2.5), page 8

Conventions

We use the following notational conventions:

- Vectors are written in boldface, e.g., $\mathbf{x}$, $\mathbf{p}$
- Operators are set in fractal, e.g., $\mathfrak{B}, \mathfrak{P}$
- Energy is measured in units of bridge rupture energy ΔE
- Distances are measured in units of grain diameter $2r$
- Definitions are written like $a \doteq b$
- With [statement] we denote the Heaviside bracket; it is 1 if the contained statement is true and 0 otherwise. With this the Delta Distribution can be written as $\delta(x-a) = [x = a]$ and the Heaviside Distribution as $\Theta(x) = [x > 0]$
- If not stated otherwise explicitly, the standard parameters in the simulations are: 10^3 runs—isoenergetically initialized with initial energy of 1000, bridge rupture distance $s_c = 0.1$, bridge rupture energy $\Delta E = 1$ and disk size 0.5

List of Figures

Chapter 1

Introduction and Fundamentals

We discuss the importance and differences between wet and dry granular matter and provide a scope for this thesis. We also elicit its connections to non-equilibrium physics and explain why simple models provide a valuable tool in studying non-equilibrium systems. Additionally, the connection taking us from microscopic laws of motion to a coarser description with the help of kinetic theory is discussed.

1.1 Overview

Understanding granular matter is important since it is ubiquitous in daily life and on a great many length-scales. These range from the microscopic scale wit grains sizes of a few microns up to a few mm[1]. On the largest scale, dry granular gases can be found in planetary rings [Spahn et al., 1995; Wallis, 1986] of Saturn or generally in the interstellar medium since distances are large compared to rock or dust diameters. Our understanding of this scale is important for, e.g., the formation of planets [Lissauer, 1993]. Dry granulates of different radius demix in gravity, famously shown by the brazil nut effect in breakfast cereals [Lissauer, 1993; Pöschel and Herrmann, 1995].
A lot of natural resources are used in powder form and the understanding of how powders behave in, e.g., silos [Luding, 1998] or drums is of interest for the industry. Additionally to static or gas phenomena, dry granulates can flow or jam. An important aspect in understanding this phenomena is that granulates posses internal structure, i.e., they consist of a large number of molecules and therefore internal degrees of freedom that we do not account for individually in our models. That means granulates posses bulk quantities like elasticity and surface roughness that can not be derived by model

[1] There are numerous definitions of what notions apply to which scale - especially among the geology community. In this work the assumption that granulates are large enough so that internal degrees of freedom do not have to be taken into account and that capillary forces are the most important attractive interaction.

equations but are considered inherent.

Also, the internal degrees of freedom are out of equilibrium with their surroundings, making it for them to absorb. Since grains loose energy by dissipation, granular matter is naturally a non-equilibrium system. This can be seen in the inelastic collapse of gases: without energy injection a granular gas is unstable with respect to the formation of clusters.

Wet granular matter adds an attractive and dissipative interaction that leads to new effects and, in itself, an interesting field of research. Consider the sandcastle: trying to make one from dry granulates results in piles. If, however, water is added the sandcastle is stable. Also its stability is largely independent on the amount of water. Alas, if one adds too much water the sand will start flowing which—on the larger scale—amounts to landslides and avalanches [Iverson, 1997]. Agglomeration of wet granulates happens, e.g., for hail stones where single ice grains coagulate [Talu et al., 2000].

From a statistical mechanics viewpoint, Fingerle and Herminghaus [2007] studied the equation of state for a wet granular gas; Fingerle et al. [2008] focused on phase transitions and Zaburdaev et al. [2006] studied free cooling of a wet granular gas in one dimension.

Additionally, the wet interaction is a good approximation to the low-energy regime of dry gases. For collisions with higher energy the granulates behave viscoelastic or vibrational modes are important. For a detailed account see, e.g., Brilliantov et al. [1996] or Aspelmeier [2000]; Schäfer et al. [1996]. We will stay at moderate energies and can neglect this regime.

Moreover, the exact shape of the attractive force-law between pairs of particles is of no consequence for some aspects. This means that a simple model of wet granulates is also able to model “sticky” gases or, in general, gases with limited, attractive interaction and dissipation to some degree [Carnevale et al., 1990; Coppex et al., 2004; Liang and Kadanoff, 1985; Trizac and Hansen, 1995; Trizac and Krapivsky, 2003]. Next to its abundance in the natural world granular matter also poses interesting problems for theoreticians: In the dilute limit of dry granulates it is a hard-sphere gas with dissipation. Therefore it is interesting to see if it can be modeled with well-known theories like the Boltzmann-equation that successfully describes gases with simple interaction. However, most of these theories have certain assumptions, e.g., molecular chaos or ergodicity [Reichl, 1980]. That such assumptions do hold has only been shown for a small set of systems (see, e.g., Simányi [2003] for some hard-sphere systems).

This puts the granular gas into the context of dynamical systems. It is easily possible to write down a Hamiltonian for model equations which in turn induces a flow. Especially the wet granular gas is interesting because it is not clear if the system can be compared to the well known hard-sphere system since, e.g., the phase space volume is not conserved by dissipative interaction. This makes it an interesting problem for the more fundamental aspects of statistical physics, like the ergodicity that is needed

by the usual means with which the Boltzmann equation is solved. Studying gases in this context is not new: during the 19th century spatial disorder of gases was first characterized by then empirical measures like entropy per unit volume. The rise of modern dynamical system ideas of dynamical chaos extended throughout the whole of the 20th century and allowed to predict transport properties (e.g. diffusivity, viscosity) in terms of microscopic dynamics. This was discovered by such famous physicists as Maxwell, Gibbs and Boltzmann (for a detailed account read e.g. Gaspard [2005] or Penrose [2003]).

However, only recently an advance in mathematical technique allowed for the study of the fundamentals of, e.g., the kinetic Boltzmann equation: Enskog extended kinetic theory too the study of dense gases in 1921 and Yvon, Bogoliubov, Born, Green and Kirkwood derived kinetic equations as an approximation from the n-particle distribution function with the BBKGY hierachy [Gaspard, 2005; Reichl, 1980].

This approach hit a few problems: expansions of this kind have problems in the non-analyticity of the particle density. Furthermore the Boltzmann equation relies on the assumption of molecular chaos and therefore on the fast decay of collision induced correlations between molecules. The time correlation functions of typical fluids show that this is not the case: they posses long-time tails as shown by Alder and Wainwright [1970]. Beijeren and Ernst [1973] proposed a modified Enskog equation that provides good results even for dense systems. For dry granular systems under shearing Montanero et al. [1999] should be mentioned: they solved the BBGKY model.

To investigate further when simple systems posses chaotic properties Sinai [1963], proved the ergodicity of a two-dimensional two-disk system.

The Sinai billiard with periodic boundary condition resembles the Lorentz gas (see e.g. Vollmer [2002]). This can be used to describe a granular gas in the limiting case of two disks. This has been done by Glassmeier [2010]. She found that this system is transiently chaotic, i.e., even if it is heated the variation of velocities is increased and the system will eventually enter a clustered, stable state with minimal energy.

For the limit of many particles in the context of dry granular gases there has been some advance in obtaining a kinetic theory: Ben-Naim et al. [2005] shows that spatially homogeneous systems show power law tails in the velocity distribution and that driven steady states with the same power law can be obtained via injecting energy at high velocities. Due to the dissipation a gas cannot be in a classical equilibrium and if no energy is injected by some means (shearing, heating, shaking) the granulates will cluster Ulrich et al. [2009a]. Nie et al. [2002] looks at the dynamics of freely cooling granular gases and analyzes the bounds of Haff's law. From the kinetic point Zippelius [2006] looked at the evolution of granular gases based on a time evolution operator for many particles and discusses the freely cooling state, as well as the correlations and energy

exchange between rotational and translation degrees of freedom. It turns out that there are correlation between the relative orientation of angular and linear velocities as shown by Brilliantov et al. [2007]. In general, the kinetic theory of dry granular gases has reached some text book level Brilliantov et al. [2003], and Pöschel and Schwager [2005], Brilliantov and Pöschel [2004]. For a seminal review the interested reader is also referred to Lun et al. [1984]

There has been some recent work on the many particle theory of wet granulates, especially by Fingerle and Herminghaus [2007] who proposes a equation of state of wet granular matter (albeit under the assumption that its dynamics is locally symplectic), Zaburdaev et al. [2006] who studied the free cooling of wet granulates and Roeller and Herminghaus [2011] who performed large scale event driven simulations of wet granulates and investigated the phase space in relation to phase transitions.

Ausloos et al. [2005] even study patterns in clusters of granulates in the context of self-organized criticality.

As a side note, for hard-sphere systems Alder and Wainwright [1970] discovered that the velocity auto correlation function decays algebraically. This can also be found in granular systems and is important for the comparison with the Lorentz gas. For this, Chernov and Markarian [2003] showed that in the finite horizon case the decay should be exponential. However, Fiege et al. [2009] confirmed the algebraic decay for sheared granular gases.

1.2 Kinetic Theory

In statistical physics we describe the dynamics of asystem with the probability density $f^{[N]}$ that assigns to each subset of the phase space $\mathbb{R}^{DN}$ a probability in $\mathbb{R}^+$, the probability to find the system in the subset[2] of finding an ensemble with particles that are in the state $(\mathbf{x}_i, \mathbf{p}_i)$. Since the probability density depends only on the canonical variables $\mathbf{x}_i$ and $\mathbf{p}_i$ its time evolution is determined by Hamilton's equation.
For a Hamiltonian $\mathcal{H}$

$$\mathcal{H} \doteq \sum_i \frac{\mathbf{p}_i}{2m_i} + \sum_{i<j} V(\mathbf{x}_i - \mathbf{x}_j) \tag{1.1}$$

[2]Note that we also normalize $f^{[N]}$ according to $\int f^{[N]} d\Gamma^N = 1$ where $d\Gamma^N$ is the measure of the ND dimensional phase space. This measure depends on the ensemble, e.g. in the microcanonical ensemble $d\Gamma^N = d\mathbf{x} d\mathbf{p}[\mathcal{H} = E]$

the equations of motions are

$$\frac{\partial p_i}{\partial t} = -\frac{\partial \mathcal{H}}{\partial x_i} \tag{1.2}$$

$$\frac{\partial x_i}{\partial t} = \frac{\partial \mathcal{H}}{\partial p_i}. \tag{1.3}$$

The time evolution of the phase space density is given by a Liouville equation

$$\frac{\partial f^{[N]}}{\partial t} = \left\{\mathcal{H}, f^{[N]}\right\}, \tag{1.4}$$

where $\{\mathcal{H}, \cdot\}$ is the Poisson bracket. The N-Particle distribution function however is difficult to use in computation. If we want to trace out some information we can reduce the phase space to $n < N$ particles by introducing the reduced phase-space distribution function

$$f^{(n)} = \frac{N!}{(N-n)!} \int f^{[N]} d\Gamma^{N-n}. \tag{1.5}$$

It describes the probability of finding a subset of n particles in the $(N-n)$-dimensional reduced phase-space. This probability does not depend on the traced-out particles. The factor $\frac{N!}{(N-n)!}$ arises from the freedom of choosing an arbitrary subset.
Using the reduced phase space density it becomes possible to relate the $f^{(n)}$ to the $f^{(n-1)}$ distribution. Repeating this hierarchy for all possible n is known as the BBGKY hierarchy. Most often the version for $n = 1$ is used

$$\left(\frac{\partial}{\partial t} + \frac{\mathbf{p}_1}{m_1}\frac{\partial}{\partial \mathbf{x}_1}\right) f^{(1)}(\mathbf{x}_1, \mathbf{p}_1; t) = -\int \mathbf{F}_{12} \frac{\partial}{\partial \mathbf{p}_i} f^{(2)}(\mathbf{x}_1, \mathbf{p}_1, \mathbf{x}_2, \mathbf{p}_2)\, d\mathbf{x}_2\, d\mathbf{p}_2 \tag{1.6}$$

with the inter-particle force $\mathbf{F}_{12}$.
Solving Equation (1.6) is problematic because it contains both the 2 and 1 particle distribution function. In the simplest approximation one assumes molecular chaos

$$f^{(2)}(\mathbf{r}_1, \mathbf{p}_1, \mathbf{r}_2, \mathbf{p}_2) = f^{(1)}(\mathbf{x}_1, \mathbf{p}_1) f^{(1)}(\mathbf{x}_2, \mathbf{p}_2) \tag{1.7}$$

For a hard-sphere gas this means that the particles behave independently from each-other.
The question to what extent the approximation is valid and to which systems it applies lies in the core of statistical mechanics. If the step in Equation (1.7) is allowed Equation (1.6) becomes a differentiable equation only in terms of the one particle distribution function. This opens the door to use a vast amount of tools from statistical physics.
As an additional remark: if only Equation (1.6) where used, we essentially neglect all 3 or more particle interactions. This approximation can only be made if the density is sufficiently low and thus pair interaction is dominant [Hansen and McDonald, 2006].

Chapter 2

Fundamentals

We discuss the force laws of dry and wet granulates and discuss which models can be used to describe these systems. Additionally, the equations of motions resulting from the model are derived which allows us to compare the granular system to the Sinai billiard. Furthermore, we introduce Lees Edwards boundary conditions as a mean to inject energy in a granular system which mimics shearing. Eventually we discuss the different methods of simulations and why we use time-driven simulations to compare small systems to Sinai billiard.

2.1 Dry and Wet Granular Interaction

In the simplest case dissipation can be described by a coefficient of restitution[1] ϵ. It quantifies the relative change in a collision between two particles with, initially, relative normal velocity $\mathbf{v}_i^n$ and, after the collision occurred, final velocity $\mathbf{v}_f$

$$\epsilon = \frac{v_f^n}{v_i^n}. \tag{2.1}$$

This relates pre- and postcollision energy (E_f, E_i respectively) by

$$E_f = \epsilon^2 E_i. \tag{2.2}$$

In general ϵ can be a more complicated function of velocity [Brilliantov and Pöschel, 2004]. Also, we ignore dissipation into the rotational degrees of freedom as this would, for now, just increase the complexity of our model[2]. In the following we discuss the

[1] Note,that our definition deviates from Glassmeier [2010] and rather instead [Brilliantov and Pöschel, 2004]. Glassmeier [2010] defines the square of ϵ as coefficient of restitution $\alpha \doteq \epsilon^2$

[2] For a review of dissipation in angular motion refer to Brilliantov and Pöschel [1998].

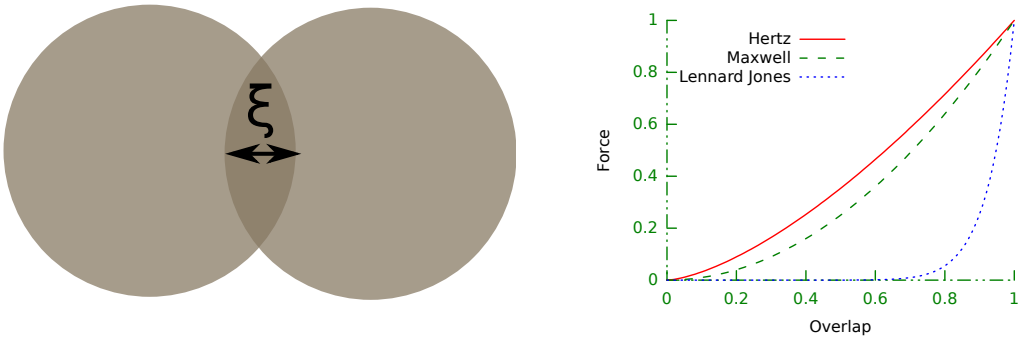

Figure 2.1 – Left: The repelling force between two granulates depends on the area-overlap and this in turn on the overlap-distance ξ defined in Equation (2.3). **Right:** The natural model for granulates is a Hertzian force that scales with $\xi^{3/2}$. Other suitable models include, e.g., a steep Lennard-Jones potential or that for Maxwell particles in two-dimensions. For comparisons to the hard-sphere model the shape of the interaction is not important. We choose the potential as steep as the Molecular Dynamics allows us. We select the Hertzian force law in accord with models commonly used for modeling dry granular matter.

main mechanisms behind granular interactions (plastic deformation, dry viscoelastic interaction, cohesive/van der Waals, wet viscous interaction, wet interaction).

Dry Interaction Viscoelastic interaction is characterized by the stress being a sum of the elastic stresses and dissipative stresses when the dissipative stress depends on the deformation rate [Landau and Lifshitz, 1975]. If deformation is slow enough this can be approximated linearly.
The force between two grains of radii r_1, r_2 at position $x_1, x_2 \in \mathbb{R}^D$ depends on the overlap ξ of particles (cf. Figure 2.1)

$$\xi \doteq r_1 + r_2 - |x_1 - x_2| \tag{2.3}$$

The disks repel each-other with a Hertzian force [Hertz, 1882] that is proportional to the overlap ξ. The proportionality between force and overlap—called the Derjaguin approximation—involves the effective radius

$$R_{\text{eff}} \doteq \frac{r_1 r_2}{r_1 + r_2}. \tag{2.4}$$

For $\xi > 0$

$$F_{el} = \frac{2Y\sqrt{R_{\text{eff}}}}{3(1-\nu^2)}\xi^{\frac{3}{2}} \tag{2.5}$$

where the Young's modulus Y and the Poisson ratio ν are material constants. Typical values for aluminium beads of size 1 mm with velocities of 30 cm/s lead to contact times in the order of μs with ξ in the order of μm [Nakagawa and Luding, 2009]. This is often used as justification for neglecting the collision dynamics and using a reflection of hard-cores in simulations.
To include viscoelastic interaction Equation (2.5) can be extended. Brilliantov et al. [1996] found

$$F_{\text{diss}} = \frac{3}{2} A \rho \sqrt{\xi}\dot{\xi} \tag{2.6}$$

where A is a material constant that depends on the grains Young's modulus Y, the Poisson ratio ν and the viscous material constants η_1, η_2 of the two particles in contact Brilliantov and Pöschel [2001].The material constant A is known for the assumption of perfectly spherical grains (also assuming that the material constants are the same for both disks which leads to $\eta_1 = \eta_2$), according to Brilliantov and Pöschel [2004]:

$$A = \frac{1}{3}\frac{4\eta^2}{5\eta}\left[\frac{(1-\nu^2)(1-2\nu)}{Y\nu^2}\right] \tag{2.7}$$

This interaction leads, since it depends on velocity and thus on time, to dissipation. From this force law alone a coefficient of restitution can be calculated (see Ramirez et al. [1999], Schwager and Pöschel [1996]) which removes a fraction of relative velocity at each collision.

Combining the two effects from Equations (2.5) and (2.6) gives

$$\ddot{\xi} + \frac{\rho}{m_{eff}}\left(\xi^{3/2} + \frac{3}{2} A \sqrt{\xi}\dot{\xi}\right) = 0 \tag{2.8}$$

However, on the scale of wet granulates the dissipation due to Equation (2.8) can be neglected if the energy is sufficiently similar to the bridge rupture energy ΔE in wet granulates: see Figure 2.2.

Wet interaction If a liquid, e.g, water is added to granular matter the liquid will aim to minimize its surface area. This can be achieved by spreading out among the granulates and covering them with a liquid film. Near the contacts of grains the shape of the liquid film becomes more complicated. Considering only liquid contents that are large enough to form toroidal liquid bridges, the surface roughness can be neglected. The force resulting from the minimization of surface area is balanced by the Laplace pressure. The Laplace pressure is a hydrostatic pressure determined by the curvature of the liquid film. This balancing leads to the formation of a liquid bridge (see Figure 2.3). This liquid bridges mediates an attractive force between the grains.
The mechanical properties of this bridges have been studied extensively by Fournier et al. [2005]; Liao and Hsiau [2010]; Mitarai and Nori [2006]; Willett et al. [2000] and in

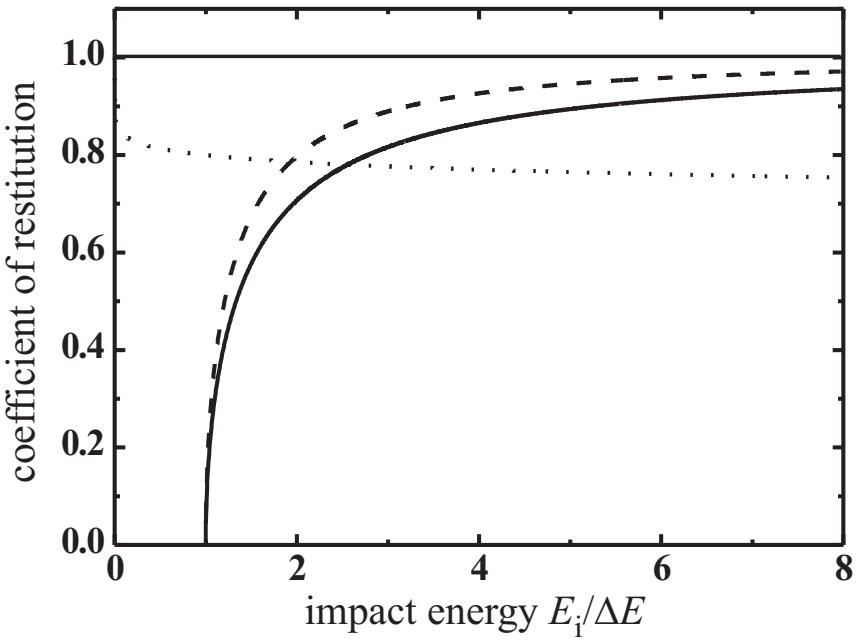

Figure 2.2 – The coefficient of restitution for dry (dotted) granulates does not introduce an energy scale. However, in the wet case (solid and dashed), there is a minimal scale at $E_i = \Delta E$. This is unchanged even if the finite formation time for capillary bridges is taken into account (dashed curve). (Figure reprinted from Ulrich et al. [2009b]).

popular form for the stability of sandcastles by Hornbaker et al. [1997]. The reasoning about the different force regimes here follow mostly the review article by Herminghaus [2005].

The exact pressure difference can be calculated for two wet granulates with radius of curvature R_1, R_2 (see Figure 2.3) by

$$p_L = \gamma(1/R_1 + 1/R_2), \tag{2.9}$$

Note, the curvature R_1 is negative and thus the pressure difference is negative too. This force drives the system towards an equilibrium once a spatially constant mean curvature has been reached.

Counter-acting the Laplace pressure is a force due to the surface tension between liquid and grain γ. The force can be calculated via Young's equation that relates the surface tension γ and the contact angle between grain and liquid ϑ

$$F_B = 2\pi\gamma r \cos\vartheta_c, \tag{2.10}$$

where θ_c is the critical wetting angle.

Solving the resulting force analytically is not possible. The consensus on an approximate force law for two particles with equal radius r is (see, e.g., Herminghaus [2005])

$$F(\xi) = \frac{F_0}{1 + 1.05\frac{r}{\hat{V}}\xi + 2.5\frac{r}{\hat{V}}\xi^2}. \tag{2.11}$$

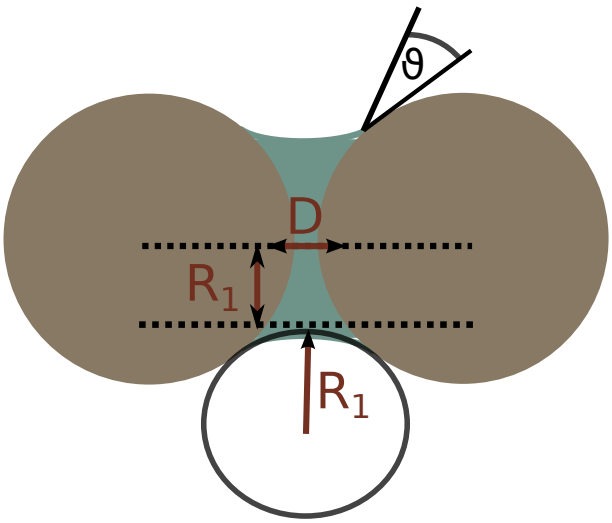

Figure 2.3 – Two spheres with identical Radius are covered by a liquid film. The liquid film contacts the sphere's surface under an angle θ. Determined by Young's equation a force is exerted on the liquid depending on the surface tension γ. This force is balanced by the hydrostatic pressure difference due to the Laplace pressure. This pressure depends on the radii of curvature R_1, R_2. Combining these forces we can obtain an approximate force law in Equation (2.11)

This compares well to experiments as convincingly done by Willett et al. [2000] , see Figure 2.4.

For this force the distance where the bridge ruptures, the rupture distance s_c can be fitted. Willett et al. [2000] obtain

$$s_c = r\left(\hat{V}^{1/3} + 0.1\hat{V}^{2/3}\right) \tag{2.12}$$

where $\hat{V}$ is a dimensionless quantity connecting the volume of fluid L and the grain volume

$$\hat{V} \doteq \frac{L}{r^3}. \tag{2.13}$$

The total energy dissipated by forming a bridge with force according to Equation (2.11) over a distance given by Equation (2.13) is the integral

$$\Delta E = \int_0^{s_c} F_{\text{bridge}} ds \approx 5.5\sqrt{\hat{V}}\gamma r^2 \cos\vartheta \tag{2.14}$$

An approximation to this can be found for complete wetting ($\cos\vartheta_c \approx 1$). Herminghaus [2005] proposes

$$\Delta E \approx \frac{2\pi\gamma}{R}\sqrt{\hat{V}}. \tag{2.15}$$

To facilitate the theoretical considerations we will use ΔE given by Equation (2.15) as energy scale and thus give all energy units in term of ΔE. Also, distances will be measured in grain diameters $2r$.

The important features that these mechanisms introduce are dissipation and stiffness

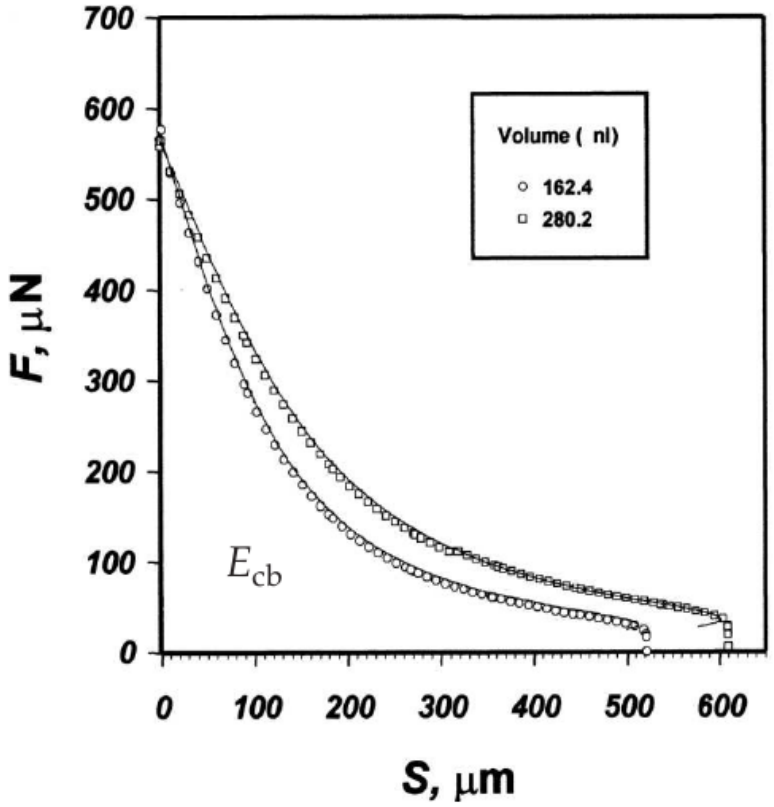

Figure 2.4 – The capillary force F between a spherical particle and a wall depends on surface separation (here, s). The force decreases monotonically with a clearly visible rupture distance.Willett et al. [2000] performed experiments with perfect wetting (points) and compared them to numerical estimate (line).
Figure reprinted from [Willett et al., 2000].

due to the attractive nature of Equation (2.11).

As an additional note, we discuss another force that gives rise to a hysteretic interaction. These are collected under the term of cohesive forces (c.f. Figure 2.5).
The Van der Waals force is the most ubiquitous cohesive force. However this type of force may be neglected for typical grain sizes $R > 20\,\mu$m. Additionally the kinetic energy scales with length-scale squared, whereas the van der Waals interaction scales with the radius [Zhu et al., 2007]. We will therefore neglect this type of interaction.
An overview of energy-scale can be found in Figure 2.6 from [Zhu et al., 2007].

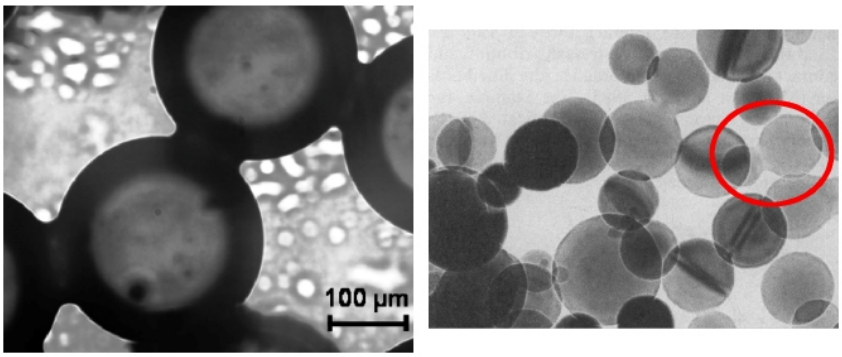

Figure 2.5 – **Left:** Water bridges have formed between glass beads. **Right:** The cohesive van der Waals force leads to necks.
Liquid bridges dominate on larger length-scales compared with $\mathcal{O}$(nm) where van der Waals forces dominate. Both interactions lead to a hysteretic potential which in turn leads to dissipation. (Pictures from Glassmeier [2010] referencing work from Scheel [2009] (**left**) and Iijima [1987] in Chokshi et al. [1993] (**right**)).

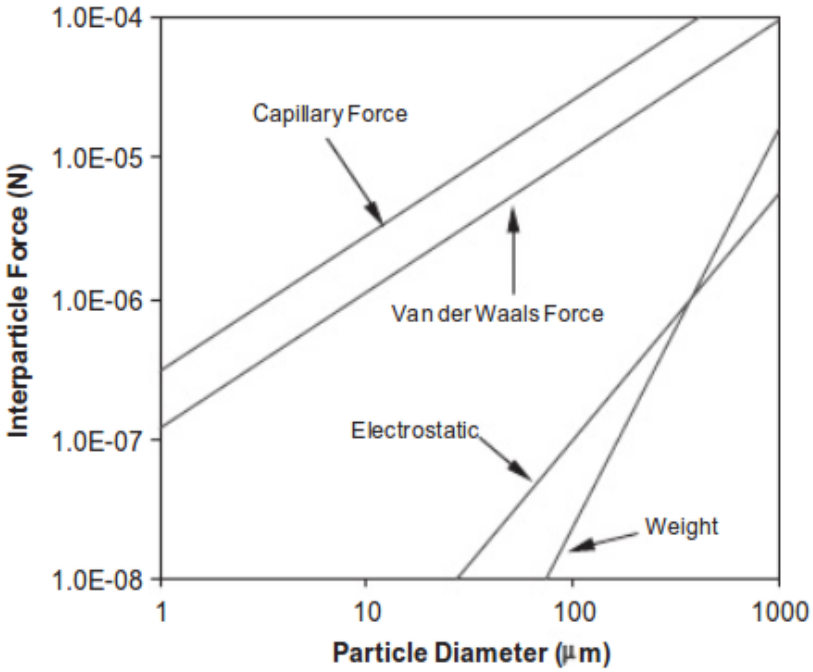

Figure 2.6 – Comparison of different inter-particle forces. The capillary force responsible for liquid bridge formation is on average half a decade stronger than the van der Waals Force for particles with sizes exceeding μm. Both of these forces are on turn a decade larger than electrostatic and weight forces.

2.2 Models for Granular Interaction

For our system there are different candidates for simple models of the microscopic interaction. First, we discuss the dry interaction between two particles. The candidates are:

Perfectly hard-spheres The interaction is defined by a infinitely steep potential. The model potential for a particle of Radius r as a function of distance to its center is

$$V(\xi) \doteq \begin{cases} 0 & \xi < 0 \\ \infty & \xi > 0 \end{cases} \tag{2.16}$$

This model is often used in Event Driven Molecular Dynamics and also by the Sinai billiard model. It is elegant in some aspects: it does neither introduce an energy nor a temperature scale and a change in energy of the whole system can be described as rescaling of the time scale. Another feature is that due to the instantaneous nature of collisions the probability for three-particle interaction is zero [Brilliantov and Pöschel, 2004]. Also, there are some problems with phase transitions: in simulations one can find a crystallization transition for high densities in three dimensions (Hoover et al. [2009]) but if this transition still exists in two dimensions is still under discussions [Mak, 2006]. Lacking attractive interactions such systems also can not show a liquid-gas transition.

Soft potentials We summarize the potentials in the form of

$$V(\xi) \doteq \begin{cases} 0 & \xi < 0 \\ \frac{1}{\xi^n} & \xi > 0 \end{cases} \tag{2.17}$$

as soft potentials. Note that the repulsive part of the Lennard Jones potential, as well as the Hertzian repulsion fall under this definition. If we want to use Molecular Dynamics we need a force law and since we are not interested in the collisions themselves we want to choose the potential as steep as the Molecular Dynamics simulations allow us. But since the force law for granulates is known to be roughly Hertzian, we will simply choose the exponent belonging to the Hertzian force law (cf. Equation (2.5)) and choose the parameters as such that the collision time and disk overlap are as small as possible. As a remark we mention that Rapoport et al. [2008] argues the Sinai billiard is chaotic, the smooth billiard possesses a stability region that scales with the steepness n of the potential like $1/n$. However we note that this is not unexpected and should not be detrimental for comparison of the hard-sphere model to the one we use in Molecular Dynamics

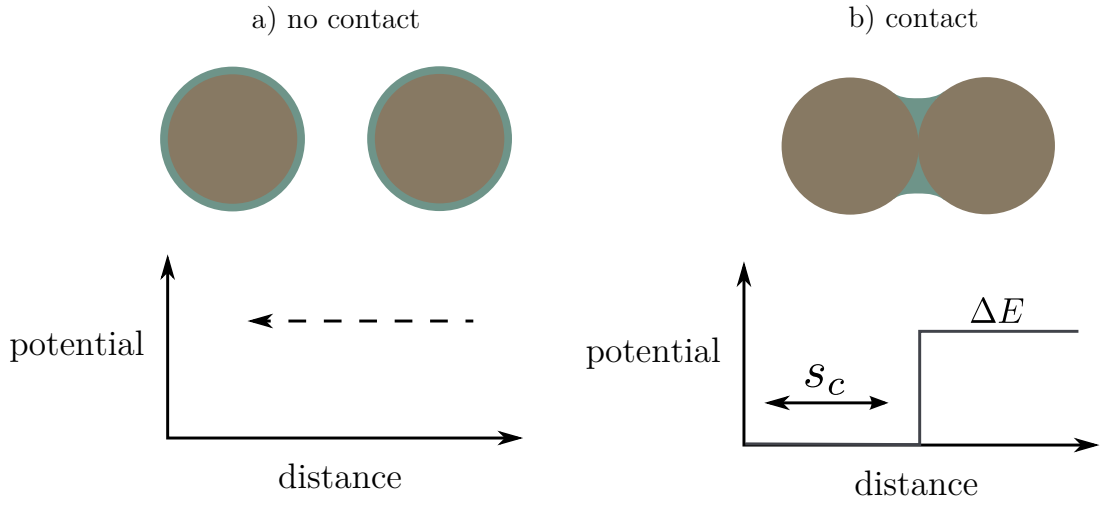

Figure 2.7 – In the thin-film model granulates move freely until they collide. They reflect then according to the repelling force model and also build a liquid bridge. In reality this bridge exerts an attracting force. However, Fingerle [2007]; Röller [2010] showed that the exact behavior of the force is not important at least for dilute granulates. Thus an easy model is to neglect the force and simply reduce the relative normal energy by ΔE of the two spheres whenever they rupture the bridge at a critical distance s_c. This implies an infinite force at rupture and can be problematic for Molecular Dynamic simulation where a force is needed. Hence, we use a smoothed out potential of the same form for our simulations where still the energy dissipation is equal to ΔE. Note that this interaction breaks time-reversibility and is dissipative. This alone is responsible for driving the granulates out of equilibrium.

simulations. Additionally, the range of our forces are small in comparison to the box length—thus we do not expect to see such contributions.

For the wet interaction especially the hysteretic nature of the force law is important. There are some natural candidates for modeling the potentials. For a direct comparison regard Figure 2.8.

Thin Film Model When two disks collide they form a liquid bridge. In the thin film model this bridge forms at contact, if the distance between the center of mass of the disks is smaller than their combined radii. After reflection the particles see a potential well that is reflecting if their relative radial velocity is smaller then the escape velocity dictated by the depth ΔE of the potential

$$V(\xi) \doteq \begin{cases} \Delta E & \xi < -s_c \quad \text{if bridge formed} \\ 0 & -s_c \leq \xi < 0 \end{cases} . \tag{2.18}$$

This model assumes that the wetting layer of liquid is infinitely small and that the force transmitted by the bridge can be infinitely large. Realistically there is a finite critical force that when transceded leads to a bridge rupture. Note that this does not allow one to store arbitrary energy into the rotation of two particles, there still is a critical energy depending on the bridge rupture energy and on the

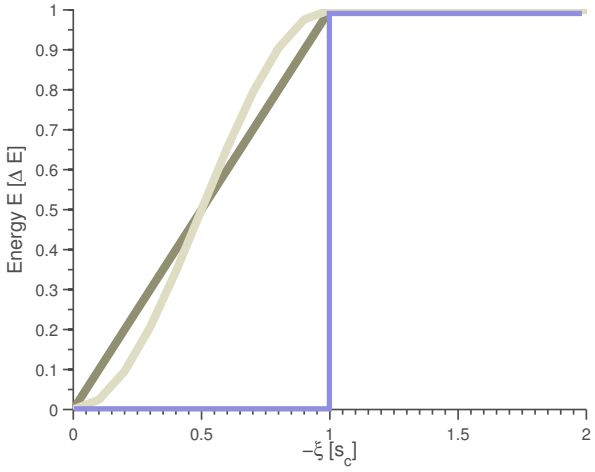

Figure 2.8 – The soft hysteretic well, constant force and thin film model describe a hysteretic pair interaction that leads to dissipation. The thin film model has a step from zero potential to the bridge rupture energy. Since the force is the derivative of the potential, it becomes infinite at the rupture distance and hence is not suited for direct integration of the equations of motion. In the constant force model this is remedied by interpolating between zero and the rupture energy linearly. However, the first derivatives behaves discontinously at the rupture distance. To obtain a continuous behavior everywhere the soft hysteretic well uses a part of the cosine for interpolation.

bridge rupture distance. Shokouhi and Parsafar [2008] discusses some properties of square well liquids.

Thick Film Model In the thick film model the assumption of a infinitely thin layer of liquid wetting the disks is relaxed. Glazing collisions will too, lead to the forming of a liquid bridge if the distance between grains is smaller then the liquid film's thickness. Glassmeier [2010] compared the thin and thick film model and notes that they equal each other in almost any aspects.

Hysteretic Constant Force For Molecular Dynamics simulations the above mentioned potential carries the disadvantage of possessing an infinite forces. A simple model with finite force in radial direction is

$$V(\xi) \doteq \begin{cases} \frac{\Delta E}{s_c}\xi & \xi < -s_c \quad \text{if bridge formed} \\ 0 & -s_c \leq \xi < 0 \end{cases} \tag{2.19}$$

Yet there is a problem that this force is discontinuous at the point of bridge rupture.

Soft Hysteretic Well To remedy the problems of the constant force model in Equation (2.19) the interaction is replaced by

$$V(\xi) \doteq \begin{cases} \frac{2\Delta E s_c}{\pi}\cos\left(\pi\frac{\xi}{2s_c}\right) & \xi < -s_c \quad \text{if bridge formed} \\ 0 & -s_c \leq \xi < 0 \end{cases} \tag{2.20}$$

The advantage is that this model has continuous derivatives everywhere. Thus we will use it.

Numerical studies comparing different force laws in different regimes (liquid, gas, solid) confirm that the thin-film model is a good approximation and the relevant parameters are the depth of the potential ΔE and the rupture distance s_c [Röller, 2010].
A model similar to this hysteretic interaction was used by Walton and Braun [1986]; Walton [1982] in the context of dry granular matter. It was used to model the viscoelasticity for high impact velocities.

2.3 Equations of Motion

We describe the motion of N spherical, mono-disperse particles in D dimensions. Their coordinates $\mathbf{x}_i \in \mathbb{R}^D$ and momenta $\mathbf{p}_i \in \mathbb{R}^D$ constitute the phase space[3]. We assume that the particle radii are equal for all particles $\forall_{i,j} r_i = r_j$. Their radii r_i are normalized to 0.5 to compare the two disk case with Glassmeier [2010]. Furthermore we set the individual particle masses m_i to one, such that momenta and velocities become equal.

[3]Note that: The phase space of the simulations and the model system that is discussed later on is compact due to periodic boundary conditions. The particle positions in this case live on the D-torus $\mathbb{T}^D$.

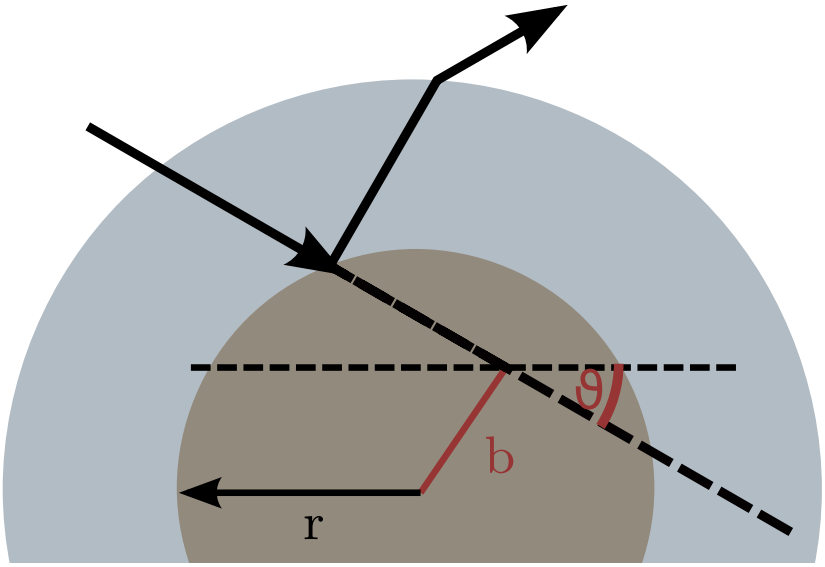

Figure 2.9 – The thin-film-Sinai billiard is described by one scatterer of double the radius of one disk. In periodic boundary conditions the other, now point-sized, disk collides elastically at the boundaries of the scatterer and is deflected at the bridge rupture distance. The coordinates b, θ allow a full description of the system since the center-of-mass-energy and time (via a Poincare section) can be eliminated as constants of motion. (Note: the energy is not constant but depends on time in a simple fashion since every collision reduces the energy by ΔE).

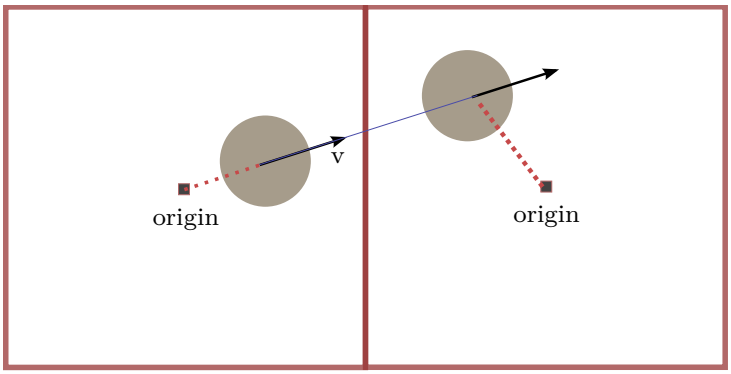

Figure 2.10 – To demonstrate that a system of disks with periodic boundary conditions does not conserve angular momentum. We consider a disk moving with a certain velocity from the direction of the origin (**left**). Its angular momentum is zero. When the disk crosses the boundary the origin is translated in such a way as to conserve linear momentum. However, if the disk reappears on the **right** it becomes apparent that the angular momentum is non-zero because of this translation. Hence, angular momentum is not conserved

Additionally, the center of mass is defined as

$$\mathbf{x}_c \doteq \frac{\sum_i m_i \mathbf{x}_i}{\sum m_i} = \frac{1}{N} \sum_i \mathbf{x}_i \tag{2.21}$$

and the total angular momentum as

$$\mathbf{L} \doteq \sum \mathbf{x}_i \times \mathbf{p}_i. \tag{2.22}$$

If we use periodic boundary conditions the center of mass velocity and the total momentum is conserved, however the angular momentum is not (see Figure 2.10). If only two disks interact in a box with periodic boundary conditions this system is known as the infinite-horizon Lorentz or Sinai billiard. It was investigated thoroughly by, e.g., Chernov and Markarian [2003]; Gaspard and Dorfman [1995]; Sinai [2007] and first adapted to wet granulates by Glassmeier [2010]. It has the remarkable property that for Sinai billiard chaoticity has been proven.

In essence the Sinai billiard describes a two particle system with periodic boundary conditions,or, from another viewpoint, one particle with zero radius moving in a lattice of scatterers with the combined radius ($r_1 + r_2 = 1$), see Figure 2.11. For the two particle system the center of mass motion is not important. Thus one eliminates it in the analysis by going to relative coordinates. In two dimensions those are $(q_1, q_2; p_1, p_2)$ and they are

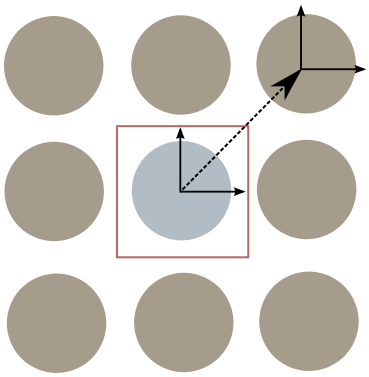

Figure 2.11 – The Sinai billiard with infinite horizon is equivalent to one point-particle moving in a lattice of disk-scatters with the combined radii of the two original disks. Crossing from one elementary box into another is equivalent to translating the origin by the box size.
This is also known as Lorentz gas.

defined by

$$q_1 \doteq x_2 - x_1 \tag{2.23}$$

$$q_2 \doteq y_2 - y_1 \tag{2.24}$$

$$p_1 \doteq m(vx_2 - vx_1) \tag{2.25}$$

$$p_2 \doteq m(vy_2 - vy_1) \tag{2.26}$$

These coordinates are not especially adapted to the evolution in the Sinai billiard. As more suitable parameters the energy (because if counting the time in collisions n the energy depends on ΔEn and we know this quantity for all n) the angular momentum (because it is related to the impact parameter) and the angle on the energy sphere of the momenta.
Vollmer [2002] describes a canonical transformation $(q_1, q_2; p_1, p_2) \to (\theta, -p; I, Q)$ to new coordinates. By specifying the above coordinates and the generating function the fourth coordinate is determined by this transformation. The complete set of new coordinates in terms of old ones is

$$I = q_1 p_2 - q_2 p_1 \tag{2.27}$$

$$Q = (q_1 p_1 + q_2 p_2)/p \tag{2.28}$$

$$p = \sqrt{p_1^2 + p_2^2} \tag{2.29}$$

$$\theta = \arctan\left(\frac{p_2}{p_1}\right) \tag{2.30}$$

The new coordinates are: Q is the projection of relative position on relative momentum normalized by the total momentum. I corresponds to the angular momentum, p is the modulus of momentum (and, since $m = 1$, the speed); θ is the direction in which the

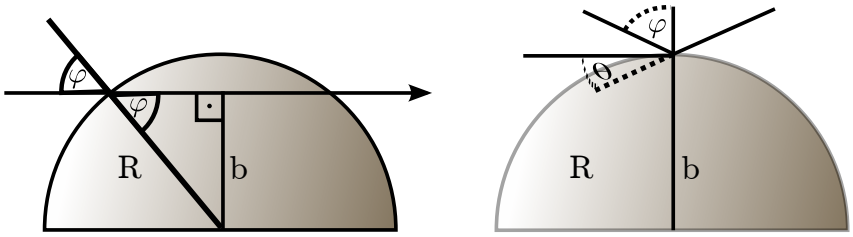

Figure 2.12 – The impact parameter b describes the distance to the point of impact. The angle of incident φ can be related to θ by noticing that $2\varphi = \Delta\theta - \pi$.

point-particle travels.
Since we have conserved quantities we can reduce the degrees of freedom:

- A Poincare section at times of collision eliminates the Q coordinate. This also implies that we loose information about how our system behaves during collisions. At the first moment this may be alarming because as we will see later on bridge rupture, collision and boundary crossings will happen at different points and at different times.
- The number of collisions determines the energy $E(n) = E_0 - n\Delta E$ and therefore $p = \sqrt{2E}$ is a strict function of n

Furthermore, for contrasting the system with classical scattering we define the impact parameter (that coincides with the one known from scattering theory) to be

$$b \doteq \frac{I}{p} \tag{2.31}$$

This leaves us with two coordinates necessary for describing the system: b, θ

We now regard the different maps namely, collision, bridge rupture, boundary crossing (see also Figure 2.9)

Collision The collision reflects the incoming particle relative to the surface normal and conserves energy. Therefore the angle θ changes according to

$$\theta \to \theta + \pi + \arcsin b \tag{2.32}$$

Periodic Boundary Crossing the boundary preserves translational invariance but destroys rotational invariance, hence angular momentum is not conserved. Crossing the boundary leads to a translation in b

$$b \to b - L\sin(\theta - \alpha) \quad \text{where} \quad \alpha \in \{0, \tfrac{1}{2}\pi, \tfrac{3}{2}\pi, \pi\} \tag{2.33}$$

Bridge Rupture First the energy is reduced according to

$$E \to E - \Delta E \tag{2.34}$$

then, since angular momentum is conserved (only a central force is exerted by the liquid bridge)

$$\sqrt{E}b = \sqrt{E'}b' \tag{2.35}$$

the impact parameter has to change like

$$b \overset{(2.35)}{\to} \frac{b}{\sqrt{1-\frac{\Delta E}{E}}} \tag{2.36}$$

We also know that

$$\sin\phi = \frac{b}{R} \tag{2.37}$$

where ϕ is

$$2\phi \doteq \theta' - \theta - \pi \tag{2.38}$$

the difference to ordinary, elastic scattering and since R does not change

$$\frac{b}{b'} \overset{(2.37)}{=} \frac{\sin\phi}{\sin\phi'} \overset{(2.35)}{=} \sqrt{1-\frac{\Delta E}{E}} \tag{2.39}$$

holds. Thus

$$\phi \to \phi' = \arcsin\frac{\sin\phi}{\sqrt{1-\frac{1}{E}}} \tag{2.40}$$

or in terms of θ

$$\theta \overset{(2.40),(2.38)}{\to} \theta + \arcsin\left(\frac{b}{(1+s_c)\sqrt{1-\frac{1}{E}}}\right) - \arcsin\left(\frac{b}{1+s_c}\right) \tag{2.41}$$

This processes can be thought of operators acting on the phase space spanned by (b,θ). The collision operator $\mathfrak{C}$ acts on (b,θ) like

$$\mathfrak{C} \circ (b,\theta) \doteq (b, \theta + \pi \arcsin b) \tag{2.42}$$

the change in phase space volume is described by the Jacobian

$$J_{ij} = \partial_i \mathfrak{C}. \tag{2.43}$$

For the collision it is given by

$$J = \begin{pmatrix} 1 & \frac{1}{\sqrt{1-b^2}} \\ 0 & 1 \end{pmatrix} \tag{2.44}$$

whose determinant is 1 since $J_{b\theta} = 0$ thus a collision only stretches the phase space volume it acts on. For the bridge rupture operator we have

$$\mathfrak{B} \circ (b, \theta) \doteq (\frac{b}{\sqrt{1-\frac{1}{E}}}, \theta + \arcsin\left(\frac{b}{(1+s_c)\sqrt{1-\frac{1}{E}}}\right) - \arcsin\left(\frac{b}{1+s_c}\right) \tag{2.45}$$

With the Jacobian

$$J = \begin{pmatrix} \frac{1}{\sqrt{1-\frac{1}{E}}} & \frac{1}{\sqrt{1-\frac{1}{E}}(s_c+1)\sqrt{1-\frac{b^2}{(1-\frac{1}{E})(s_c+1)^2}}} - \frac{1}{(s_c+1)\sqrt{1-\frac{b^2}{(s_c+1)^2}}} \\ 0 & 1 \end{pmatrix} \tag{2.46}$$

and thus the determinant

$$|J| = \frac{1}{1-\frac{1}{E}}. \tag{2.47}$$

However, this is not surprising since b is not part of the original canonical coordinates. When using I instead of b the determinant of the bridge rupture is 1 as can be readily seen by considering Equation (2.35) in which it becomes clear that the angular momentum is conserved.

Finally, the periodic boundary crossing operator $\mathfrak{P}$ is defined

$$\mathfrak{P} \circ (b, \theta) \doteq (b - L\sin(\theta - \alpha), \theta) \quad \text{where} \quad \alpha \in \{0, \frac{1}{2}\pi, \frac{3}{2}\pi, \pi\} \tag{2.48}$$

with Jacobian

$$J = \begin{pmatrix} 1 & 0 \\ -L\cos(\theta - \alpha) & 1 \end{pmatrix} \tag{2.49}$$

and thus determinant $|J| = 0$. A boundary crossing thus does not change phase space volume but shears along the b direction.
Together $\mathfrak{P}$ and $\mathfrak{C}$ shear and fold in b and θ direction. Their action on the phase space can be compared to the well studied baker map, which describes the action of stretching and folding of phase space.
In contrast to the baker map the operators $(\mathfrak{C}, \mathfrak{P}, \mathfrak{B})$ acting on the canonical variable are only invertible and volume preserving on the conditional phase space: the submanifold of constant energy. On this submanifold we can retain a "volume preserving" measure. With regard to this condition the stretching and folding leads to mixing of phase space. Glassmeier [2010] found additional structure in the non-injectivity of the bridge ruptures $\mathfrak{C}$.

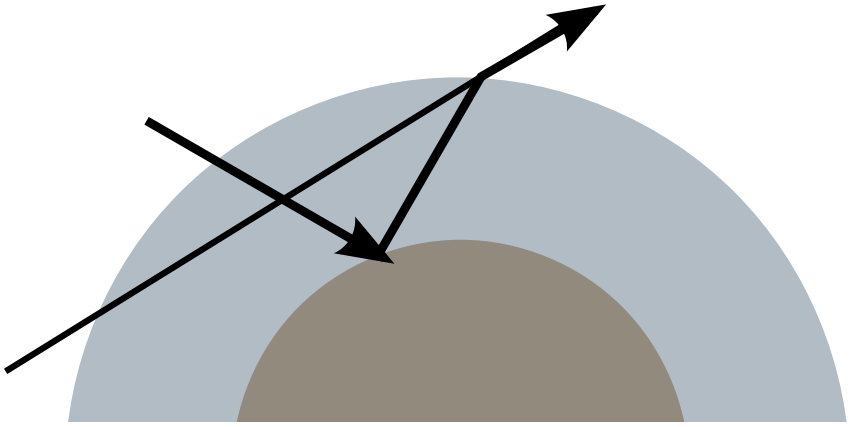

Figure 2.13 – After a reflection and bridge rupture the trajectory can not be inverted in time, since a particle that is only performing a fly-by is mapped to the same outgoing state. Glassmeier [2010] investigated the fine structuring of the phase space that results from this two-to-one-mapping

This non-injectivity is not an inherent property of the operator $\mathfrak{C}$ but rather of a collision followed by a bridge rupture since the resulting, final, state can also be obtained by a non-colliding particle. For details see Figure 2.13.

2.4 Shearing

Wet granular matter with a hysteretic potential is dissipative. A system with arbitrary initial energy will thus loose energy until a clustered low-energy state is reached. To

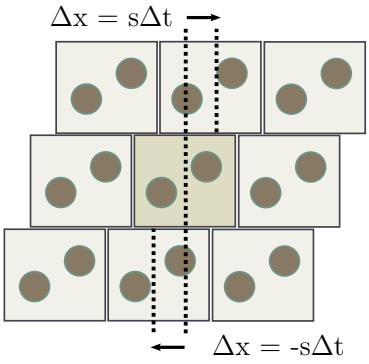

Figure 2.14 – The thin-film model is hysteretic: at each collision ΔE is lost. Too inject energy into the system we use shearing. This can be implemented easily be Lees Edwards boundary conditions. In x-direction the system still has periodic boundary conditions, but in y-direction the mirror images are moving with a shear speed s and $-s$ respectively if the disk crosses the northern or southern boundary. Since the energy is quadratic in the velocities each crossing increases the energy of the disk by $s^2/2$ on average. The energy increase does depend on the angle under which the boundary is crossed but since the billiard is hyperbolic the crossing angles are distributed uniformly.

avoid the clustered state one has to inject energy. There are different means to achieve this, e.g., thermostats, randomly picking particles and rescaling their kinetic energy. However, since in reality shear-flows are abundant, there is an additional method for energy injection: the Lees Edwards boundary conditions. They mimic a sheared system in that there are periodic boundary conditions in horizontal direction but the mirror images in vertical direction move with a velocity s, the shear speed. When a particle with velocities v_x, v_y crosses a horizontal boundary under an angle θ the energy changes according to

$$E \to \frac{1}{2}\left[(v_x \pm s)^2 + v_y^2\right] = v^2 + s^2 \pm 2s|v|\cos\theta \tag{2.50}$$

therefore the energy increase is given by the difference of the pre- and post-crossing energy (E, E')

$$E' - E \overset{(2.50)}{=} \frac{s^2}{2} - s\sqrt{2E}\cos\theta. \tag{2.51}$$

This amounts to an average increase of

$$\frac{1}{\pi}\int_0^\pi \Delta E \, d\theta = \frac{s^2}{2} \tag{2.52}$$

2.5 Simulation of Granular Systems

The main simulation methods used in granular media are Stochastic Rotation Dynamics, Lattice Boltzmann simulations, Molecular Dynamics, Direct Simulation Monte Carlo and Event-Driven Molecular Dynamics [Brilliantov and Pöschel, 2004].
Often, Molecular Dynamics simulation of granulates, especially if focus is put on their dissipative interaction, are also called discrete element simulations, DEM. The Stochastic Rotation Dynamics, Lattice Boltzmann and Monte Carlo methods are approximations that already use some assumption of molecular chaos. This is why they are not suitable to study this exact behavior.

Since we are interested in the long time behavior of small systems we do not have to deal with any sophisticated optimization techniques with regard to number of particles N since even the usual scaling of the complexity class of $\mathcal{O}(N^2)$ in calculating forces or next collisions is sufficiently fast.

Also, we want to directly solve the equations of motion. Hence, only Molecular Dynamics, or Event Driven Molecular Dynamics is suitable. The idea behind Event Driven Molecular Dynamics is to exploit the free motion of the disks whenever they are not in collision. If no external force is present it is easy to calculate the trajectory that a free particle is following and thus when the next collision occurs. These kind of

simulations are vastly faster then time driven alternatives. However, it is assumed that only pair interactions take place. Since in principle the force exerted by liquid bridges is nonzero for the bridge rupture distance, it has a finite size and for high densities three-body interaction can become important [Müller and Pöschel, 2011]. Especially since a granular gas looses energy by collisions the system will end in a clustered state where many body interactions become dominating.

The idea behind Molecular Dynamics is straightforward integration of Newton's equation of motions. For those, several good numerical solvers are known (Euler, Runge-Kutta to name the most prominent).

The complete Discrete Element Method or Molecular Dynamics method we use can be easily summarized by the following algorithm

```
1  Given: Particle positions, velocities, time and run-time T
2         time-step Δt
3  t = 0
4  while t < T do
5    for all particles do
6      find interacting particles
7      compute forces
8    end for
9    for all particles do
10     integrate equations of motion
11     update boundary conditions
12   end do
13   t = t + Δt
14 end while
```

Additionally the system's state (e.g. the disk coordinates, average kinetic energy) is written out in pre-defined time-intervals and on top of that every few collisions. The exact details depend on the number of collisions per time and thus changes depending on initial energy or - in sheared systems - depending on the shear rate.

Since we are interested in the dynamics of phase space volumes we have to be careful since they do not preserve this volume [Frenkel and Smit, 2002]. Therefore we use a symplectic integrator: the Velocity Verlet method.

The advantage of the Verlet algorithm, which is a simple form of a truncated Taylor series approximation, is that it preserves volume and is also numerically stable. For

dissipative systems one actually prefers the Velocity Verlet method, since its use allows to utilize velocity dependent forces. It can be summarized.

```
Given: Positions x_i, accelerations a_i, velocities v_i, forces
    f_i, masses m_i and time-step Δt
for i = 0,N do
    x_i = x_i + v_i + (1/2) a_i (Δt)^2
    v_i = v_i + a_i (1/2) Δt
    a_i = f_i / m_i
    v_i = v_i + a_i (1/2) Δt
end for
```

The disadvantage is however, that the time-step Δt can not be adapted. This is crucial for simulating steep potentials: In the vicinity of steep changes in the potential - for comparing with hard-sphere models - the time-step has to be small because the forces acting are large. On the other hand, if disks are not in contact, this time-step is much too small.
Also, for sheared systems the energy can vary over several decades, thus the time-step has to be adapted.
With this in mind, there are several integrator schemes of higher order than the Velocity Verlet that deal with this problem. Often used in Molecular Dynamics is the 4th-order Gear-Adams integrator. The problem with this algorithm is that it is not a symplectic integrator: it does not conserve phase space volume. Thus we used the Velocity Verlet scheme for the free cooling systems and the checks for uniformity of phase space and cross checked this with the Gear-Adams integrator we need to simulate sheared systems in reasonable time. It turns out that numerical errors are unnoticeable small for the large number of systems we use (more than 1000)[4].

Another important implementation point are the boundary conditions. When studying the system in free cooling we use periodic boundary conditions. Since the forces we use have a natural cutoff the implementation is easy: If, e.g., the distance between two disks in x-direction exceeds half the box length $L_x/2$ then the box length is subtracted from this distance until it is smaller.

In contrast, implementing the Lees Edwards boundary conditions is more involved. They are used to inject energy by implementing a kind of shearing [Lees and Edwards, 1972]. If a disk with velocity $\mathbf{v}$ crosses the boundary, its velocity is changed to $\mathbf{v} \pm s\hat{x}$, in the direction of the unit vector $\hat{x}$. Also, given the simulation time passed t, the disk is translated from its former position at $\mathbf{x}$ to $\mathbf{x} \pm st\hat{x}$.

[4] For a detailed discussion on the merit of different integrator schemes see [Dullweber et al., 1997; McLachlan and Atela, 1992]

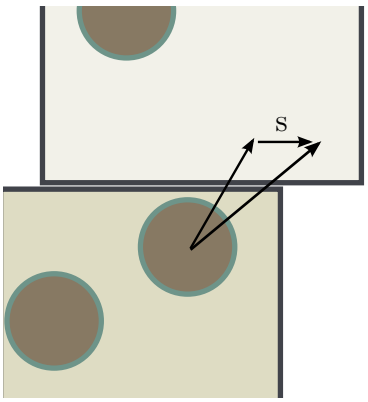

Figure 2.15 – In Lees Edwards boundary conditions the upper and lower boundaries are moving with a shear velocity $\pm s$. If a disk crosses the boundary, the shear speed s is added to the x-component of its velocity and it is translated. The translation is due to the moving coordinate frame.
Also, if a collision over a boundary occurs the relative velocity has to be corrected with regard to the moving coordinate frame.

Additionally, if disks interact across a Lees Edwards boundary we have to consider that both disks see each-other from a moving frame of reference. Thus, when computing interactions over a boundary we have to account for the translation, and the moving frame of reference, see also Figure 2.15. Additionally, if the system is sheared and the energy injection is positive, i.e., if the particles gain more energy by crossing the Lees Edwards boundary than by loosing energy in collisions, the average energy increases. For long simulation times we then have to adapt the time-step δt since for high energies the relative velocities are higher as well. That means we have to resolve the steep potential better for getting accurate results. On the other hand, for low energies, the time-step can be larger, thus again saving time in simulation. A good approach is to set $\Delta t = 10^{-4} \cdot \max(\|v\|)$ every 10^2–10^3 collisions.

Chapter 3

Small Conservative Systems

We discuss the statistical physics of small, conservative systems and provide the distribution functions for energy, momentum and relative momentum. Additionally, we investigate how periodic boundary conditions affect these distribution.

3.1 Prelude

In classical statistical mechanics we look at well known ensembles from which we obtain approximations to our systems. However, in small systems with periodic boundary conditions there are some differences to account for:

(a) Corrections to distributions for small number of particles, e.g. $N < 10$, are noticeable

(b) Because of periodic boundary conditions angular momentum is not conserved for $N > 2$ particles

(c) Even though linear momentum is conserved

The following, mostly technical discussion, will be kept brief and relevant to our system. If the reader is interested in a more detailed discussion, the texts of Huang [1987]; Reichl [1980] are recommended.
Given a fixed number of particles N, fixed system volume V and initial energy E the relevant ensemble is the microcanonical ensemble with the partition function Q_{NVE}

$$Q_{NVE} = \sum_{\Gamma} [\mathcal{H} = E] \overset{(3.2)}{=} \frac{1}{N} \frac{1}{(2\pi)^{DN}} \int [\mathcal{H} = E] \, d\Gamma \tag{3.1}$$

where Γ is the phase space volume defined by

$$d\Gamma = dx^{DN} dp^{DN} \tag{3.2}$$

As an aside, since for large number of particles the volume of an N-sphere is centered around its surface one replace the delta-function in Equation (3.1) by $[\mathcal{H} < E]$, a Heaviside-function. Another justification for this is the invariance of phase volume to changes of external parameters [Pearson et al., 1985]. This energy-shell volume is defined by

$$\Omega_{NVE} \doteq \int_0^E Q_{NVE} dE. \tag{3.3}$$

To obtain statistical quantities one has to perform the integration in Equation (3.1). Khinchin [1949] obtained

$$Q_{NVE} = \frac{2(2\pi E)^{DN/2}}{dN\Gamma(DN/2)} \left(\Pi_{i=1}^{N} m_i^{D/2}\right) \frac{Z(N,V)}{(2\pi)^{DN}} \tag{3.4}$$

where $Z(N,V)$ is the hard-sphere configuration integral [Reichl, 1980]. This is the basis for calculating different observables. We, however are more interested in the energy and velocity distribution function.
Graben and Ray used Equation (3.4) to compute the one-particle momentum distribution by tracing out all momenta and coordinates except the momentum $\mathbf{p}_1$

$$P(N,V,E,\mathbf{p}_1)\, d\mathbf{p}_1 = \frac{\Gamma(DN/2)}{\Gamma(D(N-1)/2)(2\pi m_1 E)^{D/2}} \left(1 - \frac{\mathbf{p}_1^2}{2m_1 E}\right)^{[D(N-1)/2]-1} [E > \frac{\mathbf{p}_1^2}{2m_1}]\, d\mathbf{p}_1 \tag{3.5}$$

From which one can obtain by change of variables $E = \mathbf{p}_1^2/2(m)$ the one-particle energy distribution

$$P(N,V,E,E_0)\, dE = \frac{\Gamma(DN/2)}{\Gamma(D/2)\Gamma(d(N-1)/2)} \left(\frac{E}{E_0}\right)^{D/2} \left(1 - \frac{E}{E_0}\right)^{d(N-1)/2-1} \frac{1}{E} [E < E_0]\, dE \tag{3.6}$$

As a side note: by performing the limit $N \to \infty, E \to \infty$ one obtains with

$$\frac{E}{N} = dk_B T/2 \tag{3.7}$$

the classical Maxwell Boltzmann distribution

$$P_{\text{Boltzmann}}(E_1) = \frac{(k_B T)^{-d/2}}{\Gamma(D/2)} E_1^{d/2-1} \exp(-E_1/(k_B T)). \tag{3.8}$$

Equation (3.6) does describe the hard-sphere gas for small systems. This works well for reflecting boundary conditions, yet, if one wants to minimize the effects from walls one uses periodic boundary conditions. These however introduce constraints in the form of a conserved center of mass motion. Denote by P the total momentum and v_{ij} the jth

velocity component of the ith particle, then there are $2d$ constraints

$$P_j = \sum_i^N m_i v_{ij} \tag{3.9}$$

and the position of the center of mass G

$$G_j = M_{tot}^{-1}\left[P_j t - \sum_i^N m_i(r_{ij}(t) + \sigma_{ij})\right] \tag{3.10}$$

The quantity σ is a d-dimensional vector that describes the repeating-cell lattice vector to which the ith particle moves in time t and is included such that G does not behave discontinuous while crossing a boundary. These constraints have to be incorporated into the partition function Equation (3.1)

$$Q_{NVEPG} = \frac{1}{N}\frac{1}{(2\pi)^{dN}}\int [\mathcal{H} = E][P = \sum_i^N P_i][G = M_{tot}^{-1}\left(Pt - \sum_\sigma \sum_i^N m_i r_i(t)\right)]d\Gamma \tag{3.11}$$

From here, Shirts et al. [2006] performed the integration of Equation (3.11) and obtained the one particle energy distribution given that the whole system has an energy E_0

$$P_d(N,V,E_0,E)dE = \frac{\Gamma\left(\frac{d(N-1)}{2}\right)}{\Gamma\left(\frac{d}{2}\right)\Gamma\left(\frac{d(N-2)}{2}\right)}\left(\frac{E}{E_0\frac{N-1}{N}}\right)^{d/2}\left(1-\frac{E}{E_0\frac{N-1}{N}}\right)^{d(N-2)/2-1}\frac{1}{E}[E < E_0\frac{N-1}{N}]\,dE \tag{3.12}$$

Moreover, for the relative momentum distribution we can obtain

$$P(N,V,E,\mathbf{p}_1,\mathbf{p}_2) \;=\; \frac{\Gamma(D(N-1)/2)}{\Gamma(D(N-3)/2)(2\pi m_{\text{eff}}E)^D}[E > E_{12}]\left(1-\frac{E_{12}}{E}\right)^{D(N-3)-1} \tag{3.13}$$

where, with the total mass $M_{\text{tot}} \doteq \sum_i m_i$,

$$E_{12} \doteq \frac{(m_2\mathbf{p}_1 - m_1\mathbf{p}_2)^2}{2m_1m_2(m_1+m_2)} + \frac{M_{\text{tot}}(\mathbf{p}_1+\mathbf{p}_2)^2}{2(m_1+m_2)(M_{\text{tot}}-m_1+m_2)^2}. \tag{3.14}$$

Additionally, the effective mass m_{eff} is defined by

$$m_{\text{eff}} \doteq \left(\frac{m_1m_2(\sum_i m_i - m_1 - m_2)}{\sum_i m_i}\right)^{1/2} \tag{3.15}$$

In our case we can simplify this as all masses are equal and normalized to 1, the total momentum is 0. With this simplifications we obtain

$$E_{12} = \frac{(\mathbf{v}_1 - \mathbf{v}_2)^2}{4} + \frac{(\mathbf{v}_1 + \mathbf{v}_2)^2}{4} \tag{3.16}$$

$$m_{\text{eff}} = \sqrt{\frac{N-2}{2}} \tag{3.17}$$

therefore

$$\begin{aligned} P(N,V,E,\mathbf{v}_1,\mathbf{v}_2) \quad = \quad & \frac{\Gamma(D(N-1)/2)}{\Gamma(D(N-3)/2)(2\pi\sqrt{\frac{N-2}{2}}E)^D}[E > \tfrac{(\mathbf{v}_1-\mathbf{v}_2)^2}{4} + \tfrac{(\mathbf{v}_1+\mathbf{v}_2)^2}{4}] \\ & \cdot\left(1 - \frac{\frac{(\mathbf{v}_1-\mathbf{v}_2)^2}{4} + \frac{(\mathbf{v}_1+\mathbf{v}_2)^2}{4}}{E}\right)^{D(N-3)-1} d\mathbf{v}_1\, d\mathbf{v}_2 \end{aligned} \tag{3.18}$$

For easier use the different distributions in the NVEPG-Ensemble are summarized in Table 3.1.

In later calculations we are additionally aided by the calculations of the n-th moment of the velocity distribution. Shirts et al. [2006] provide

$$\langle v_{\text{rel}}^k \rangle_{NVEPG} = \frac{\Gamma((D+k)/2)\Gamma(D(N-1)/2)}{\Gamma(D/2)\Gamma((D(N-1)+k/2))}\left(\frac{2NE}{N-1}\right)^{k/2}. \tag{3.19}$$

With this[1] we have everything to calculate averages for small granular systems.

In the Maxwellian limit we should be able to retain the collision frequency and relative velocity known from literature. The relation between $\langle v \rangle$ and $\langle v_{rel} \rangle$ is in most cases a simple one. An intuitive deviation relates $\int v f(v)\, dv$ to $\int \|v_{rel}\| f(v_1, v_2)$ by noting that the absolute value is defined by $\|v_{rel}\| = \sqrt{(\|v_2\| - \|v_1\|)^2}$ and if we neglect correlations in the square root as well as assuming molecular chaos $v_1 v_2 = 0$ and $f(v_1, v_2) = f(v_1) f(v_2)$. Thus we have

$$\langle v_{rel} \rangle \approx \sqrt{2}\langle v \rangle. \tag{3.20}$$

For a more detailed discussion, Shirts et al. [2006], provide the complete calculation and a comparison of $\langle v_{rel} \rangle$ and $\langle v \rangle$—we only note that we neglected not only correlations but also assumed the disk masses to be equal.

From Equation (3.19) we get[2]

$$\lim_{N,E\to\infty,\infty} \langle v_{\text{rel}} \rangle_{NVEPG} = \sqrt{2kT}\frac{\Gamma((1+D)/2}{\Gamma(d/2)} = \begin{cases} \sqrt{\frac{8kT}{\pi}} & D = 3 \\ \sqrt{\frac{\pi kT}{2}} & D = 2 \end{cases} \tag{3.21}$$

[1] To check the trustworthiness of this claim, we insert example numbers for the Sinai billiard. For $D = 2, N = 2$ the average relative velocity is $2\sqrt{E}$ which is what we expect.

[2] Checked by Mathematica

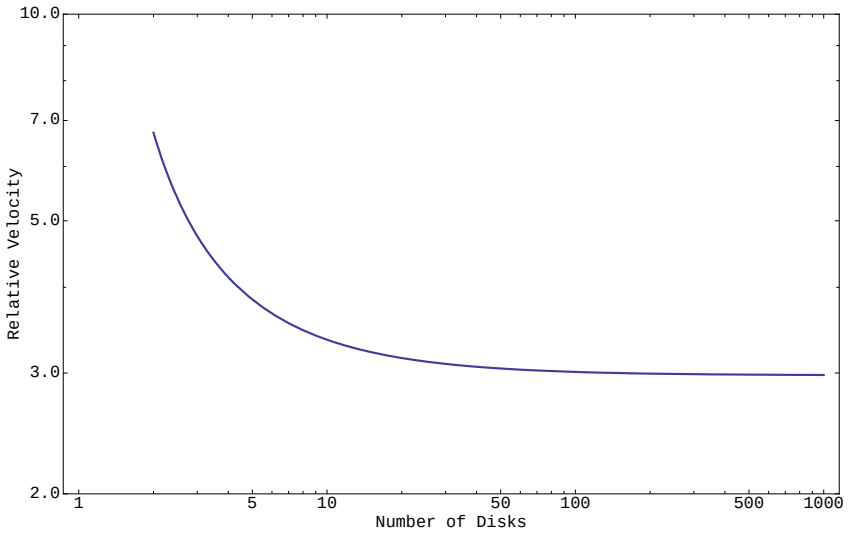

Figure 3.1 – Relative velocity from Equation (4.51) for $D = 2$ with normalized y-axis in units of kT. In this double logarithmic plot the relative velocity converges rapidly to its $N \to \infty$ limit value. From approximately $N = 10$ upwards the deviations are nearly negligible.

Comparing Equation (3.21) with classical statistical physics [Reichl, 1980] and Brilliantov and Pöschel [2004] this matches nicely.
Finally we note that Equation (3.19) converges rapidly for increasing N—this can be seen in Figure 3.1.

probability distribution	
momentum	$\frac{\Gamma(D(N-1)/2)}{\Gamma(D(N-2)/2)(2\pi(N-1)/NE)^D}[E > \frac{v^2}{2}\frac{N}{N-1}]\left(1-\frac{v^2}{2E}\frac{N}{N-1}\right)^{D(N-2)/2-1}$
energy	$\frac{\Gamma(D(N-1)/2)}{\Gamma(D/2)\Gamma(D(N-2)/2)}\left(\frac{E}{E_0}\right)^{d/2}\left(1-\frac{E}{E_0}\right)^{D(N-2)/2-1}\frac{1}{E}[E < E_0]$
relative momentum	$\frac{\Gamma(D(N-1)/2)}{\Gamma(D(N-3)/2)(2\pi\sqrt{\frac{N-2}{2}}E)^D}[E > \frac{(\mathbf{v}_1-\mathbf{v}_2)^2}{4}+\frac{(\mathbf{v}_1+\mathbf{v}_2)^2}{4}]\left(1-\frac{\frac{(\mathbf{v}_1-\mathbf{v}_2)^2}{4}+\frac{(\mathbf{v}_1+\mathbf{v}_2)^2}{4}}{E}\right)^{D(N-3)-1}$

Table 3.1 – Probability Distributions in NVEPG ensemble.

Chapter 4

Free Cooling

We derive under which conditions wet granular disks form clusters. The clustering probability turns out to be a function of the relative energy distribution. We derive the probability of clustering. As an example of how this can be applied to a coarser description we propose corrections to Haff's law that describes the free cooling of a granular gas. Eventually, we discuss the simulation of wet granulates for a small number of disks and compare them to the wet Sinai billiard.

4.1 Clustering

In this section we aim to understand the cluster formation of a freely cooling granular system. Let us therefore consider two disks: they form a cluster if the radial energy $E_{rad,c}$ with respect to their center of mass is smaller than the escape energy (i.e. the energy needed for the liquid bridge to rupture)

$$E_{\mathrm{rad,c}} < \Delta E \tag{4.1}$$

For obtaining an expression for the radial energy we note that the whole center of mass energy can be divided into the radial and tangential part—$E_{\mathrm{rad,c}}, E_{\mathrm{tan,c}}$ respectively—by

$$E_c = E_{\mathrm{rad,c}} + E_{\mathrm{tan,c}}. \tag{4.2}$$

With respect to the collision angle ϕ (see Figure 2.12) this gives

$$E_c = E_c \cos^2\phi + E_c \sin^2\phi \tag{4.3}$$

Now we know that in a bridge rupture the impact parameter b changes according to

$$b \to \frac{b}{\sqrt{1-\frac{1}{R}}}. \tag{4.4}$$

With the following identity

$$\cos^2\phi = 1 - \sin^2\phi \tag{4.5}$$

and the fact that

$$\sin^2\phi = \frac{b^2}{(R+s_c)} \tag{4.6}$$

we get the expression

$$\cos^2\phi \overset{(4.5)}{=} 1 - \sin^2\phi \tag{4.7}$$

$$\overset{(4.6)}{=} 1 - \frac{b^2}{(R+s_c)^2}. \tag{4.8}$$

Using this we obtain

$$E_{\text{rad,c}} \overset{(4.3),(4.8)}{=} E\left(1 - \frac{b^2}{(R+s_c)^2}\right). \tag{4.9}$$

For clustering to occur the condition from Equation (4.1) has to be satisfied

$$E_{\text{rad,c}} = E\left(1 - \frac{b^2}{(R+s_c)^2}\right). \tag{4.10}$$

This gives a bound on a critical center of mass energy

$$E_{\text{crit}} < \frac{\Delta E}{\left(1 - \frac{b^2}{(R+s_c)^2}\right)} \tag{4.11}$$

Assuming a flat distribution of b we can hence obtain the clustering probability

$$P(cl|E_s) = \begin{cases} 1 & [E_s < \Delta E] \\ 1 - (1+s_c)\sqrt{1-\frac{1}{E}} & E \in [1, E_{\text{crit}}] \\ 0 & \text{else} \end{cases} \tag{4.12}$$

We can additionally exploit that total energy is given in terms of number of bridge ruptures n to express the "time-dependent"-energy E_n

$$\sum E_n = E_0 - n\Delta E. \tag{4.13}$$

In the two-particle case Equation (4.12) gives us directly the result for the clustering rate. However, in the $N > 2$ particle case the center of mass energy of two disks depends

on the one-particle energy. This one-particle energy is again distributed according to a probability distribution that we either put in via initial conditions or which relaxes to an equilibrium distribution after some collisions.

From Table 3.1 we know the energy distribution. In the $N = 3$ case the energy distribution is—for the first time—non-trivial. It is a uniform distribution

$$p(E_s) = \frac{1}{E_0 - n\Delta E}[E_s < E_0 - n\Delta E] \tag{4.14}$$

The relative energy between two disks is given by

$$\frac{1}{2}(\mathbf{v}_1 - \mathbf{v}_2)^2 = v_1^2 + v_2^2 - 2\mathbf{v}_1\mathbf{v}_2 \tag{4.15}$$

in the average over the angle between two disks the third term on the r.h.s. equals zero if we can neglect any correlation due to previous collisions. We do this here exemplary for the three particle case:

$$E_s \doteq \langle E_s \rangle 2(E_1 + E_2) \tag{4.16}$$

Since the E_i are random variables their pdf changes according to a convolution if we assume molecular chaos

$$p(E_s) = \frac{1}{2} p(E_i) \star p(E_i) \tag{4.17}$$

we get

$$p(E_s) \overset{(4.12)}{=} \frac{1}{2}\left(\frac{1}{E_0 - n\Delta E}\right)^2 \int_0^\infty [E_i < E_0 - n\Delta E][E_i - E_s < E_0 - n\Delta E] dE_i \tag{4.18}$$

$$\overset{\text{part. int}}{=} -\frac{1}{2}\left(\frac{1}{E_0 - n\Delta E}\right)^2 \int_0^\infty (E_0 - n\Delta E)[E_i = E_s = E_0 - n\Delta E) dE_i \tag{4.19}$$

$$= -\frac{1}{2}\frac{1}{E_0 - n\Delta E}(E_0 - n\Delta E + E_s) \tag{4.20}$$

In general we have to calculate the conditional probability $P(cl)$. We will calculate it and compare it to Equation (4.20):

$$P(cl) = \int P(cl|E_s) P(E_s) dE_s \tag{4.21}$$

We need the distribution $P(E_s|E_s = 1/2v_{rel}^2)$. We obtain this by calculating

$$\int_{\mathbb{R}} P(v_{rel})[E_s = \frac{1}{2} v_{rel}^2]. \tag{4.22}$$

The Delta Distribution in Equation (4.22) transforms like

$$[h(x) = 0] = \sum_i \frac{[x = x_i]}{h'(x_i)}. \tag{4.23}$$

Since $[E_s = \frac{1}{2}v_{\text{rel}}^2]$ has two solutions we have to use Equation (4.23) to obtain

$$P(E_s) = \frac{2}{\sqrt{2E_s}} P_{v_{rel}}(\sqrt{2E_s}) \tag{4.24}$$

where we used that $P(v_{\text{rel}})$ is an even function in v_{rel}
Before being able to insert the distribution function from Equation (3.18) into Equation (4.24) we must note that we have to bring it in a different form, since it still depends on $\mathbf{v}_1, \mathbf{v}_2$ in Equation (3.18):

$$\begin{aligned} P(N, V, E, \mathbf{v}_1, \mathbf{v}_2) \quad = \quad & \frac{\Gamma(D(N-1)/2)}{\Gamma(D(N-3)/2)(2\pi\sqrt{\frac{N-2}{2}}E)^D}[E < \frac{(\mathbf{v}_1-\mathbf{v}_2)^2}{4} + \frac{(\mathbf{v}_1+\mathbf{v}_2)^2}{4}] \\ & \cdot\left(1 - \frac{\frac{(\mathbf{v}_1-\mathbf{v}_2)^2}{4} + \frac{(\mathbf{v}_1+\mathbf{v}_2)^2}{4}}{E}\right)^{D(N-3)-1} d\mathbf{v}_1\, d\mathbf{v}_2 \end{aligned} \tag{4.25}$$

Introducing $\vec{\alpha} \doteq \mathbf{v}_1 - \mathbf{v}_2$ and $\vec{\beta} \doteq \mathbf{v}_1 + \mathbf{v}_2$ the non-constant part of Equation (4.25) becomes

$$\int_{\alpha=-\sqrt{4E-\beta^2}}^{\alpha=-\sqrt{4E+\beta^2}} [4E < \beta^2]\left(1 - \frac{\alpha^2+\beta^2}{E}\right)^{D(N-3)-1} \alpha^{D-1}\, d\alpha d\theta \tag{4.26}$$

where we introduced spherical coordinates $d\vec{\alpha} = \alpha^{D-1} d\theta$. Integrating over θ yields the volume of the $D-1$-sphere

$$\int_{D-1 \text{ sphere}} = \frac{\pi^{D/2}}{(D/2)!} D. \tag{4.27}$$

This, together with integrating over $d\alpha$ leads to

$$\begin{aligned} & \pi^{D/2}/(D/2)!D(2^{-2+D\left(-\frac{7}{2}+n\right)}e^{1+2D-DN}(-2+N)^{-D/2}\pi^{-\frac{1}{2}-D} \\ & \left(e - v^2/2\right)^{-1+D(-2+N)}\Gamma\left[\tfrac{1}{2}+D\right]\Gamma\left[\tfrac{1}{2}(1+D(-3+N))\right]\Gamma\left[\tfrac{1}{2}D(-1+N)\right])/\Gamma\left[\tfrac{1}{2}+D(-2+N)\right]. \end{aligned} \tag{4.28}$$

As an example let us consider the case of $D = 2, N = 3$. Inserting this into Equation (4.28) we obtain

$$\frac{(E - v^2/2)}{\sqrt{2}E}. \tag{4.29}$$

Or, in terms of relative energy E_s, with respect to Equation (4.24)

$$\frac{E - E_s}{2E} \tag{4.30}$$

Not surprisingly, this gives the same result as in Equation (4.20).

This allows us to compute, in dependence of the system's energy, for example the probability of a two particle cluster in a three particle system. We compute this for the three particle clustering

$$p(cl) = \int dE_S \frac{E-2E_s}{E} \begin{cases} 1 & [E_s < 1] \\ 1 - 1.1\sqrt{1-\frac{1}{E_S}} & E \in [1, E_{crit}] \\ 0 & \text{else} \end{cases} \tag{4.31}$$

For $\Delta E = 1, s_c = 0.1$ the critical energy E_c becomes $E_c = 5.76$. The integral consists additively of the three cases. They can be integrated separately to obtain

$$P(cl) = 2.88 - 2.618\sqrt{\frac{-1+\mathrm{E}}{\mathrm{E}}} + \frac{8.84884\sqrt{-1+\mathrm{E}}}{\mathrm{E}^{3/2}} - \frac{8.2944}{\mathrm{E}} \tag{4.32}$$

This means, that even in the limit of large systems there is still a chance of bridges to occur. However, the third particle may free the two-particle cluster. For the whole system to cluster there has to be a two-particle cluster with probability given by Equation (4.32) and additionally the third particle has to have a small enough energy relative to the two-particle cluster.
If we consider Equation (4.32) in the limit of large energies and many particles with $E = 1/2NkT$, then the probability of the whole system to cluster is given by

$$P(\text{clustered system}) \approx \lim_{N\to\infty} P(cl)^N = (0.738)^N \tag{4.33}$$

When the number of particles grow large in Equation (4.33) the probability of clustering the whole system becomes zero if the system energy is larger then bridge rupture energy and 1 if it is smaller.
In the simulations we will see this behavior confirmed in Figure 4.4.

4.2 Haff's Law

To study free cooling it is useful to introduce an easy to compute observable that measures the average energy in the system. For granular matter one can define a granular temperature. This is not a temperature in the thermodynamic sense since granular matter is inherently out of equilibrium and even there shows some unexpected behavior [Kleider, 2012]. We define the granular temperature T as average kinetic energy per particle

$$T \doteq \frac{2}{D}\frac{1}{N}\sum_{i=1}^{N}\frac{1}{2}m_i\mathbf{v}_i^2. \tag{4.34}$$

To describe the change of granular temperature over time we look at the average loss of energy per unit time

$$\Delta E_{\text{tot}} = \Delta E \frac{N f_{\text{coll}} \Delta t}{2} P_{bb} \tag{4.35}$$

this means: the change in energy depends on the number of particles N, the frequency of their collisions f_{coll} and the time step Δt as well as the probability that a collision results in a bridge rupture and not in a 2 particle cluster that persists. Ulrich et al. [2009a] argue that the collision frequency depends on the scattering cross-section $\sigma = \pi d^2$, the number of particles per volume $n \doteq \frac{N}{V}$ and the square root of the temperature (for unit mass temperature has units of velocity squared—thus the square root of this equals the average velocity)

$$f_{\text{coll}} \doteq 4 g(d) \sigma n \sqrt{\frac{T}{\pi m}} \tag{4.36}$$

the remaining $g(d)$ is the two particle correlation function.This can be rationalized the following way: A particle moving with the average relative velocity $\bar{v}_{12}$ traverses a cylinder of length $\bar{v}_{12}\delta t$ in a time δt with volume $\pi\sigma^2$. Together with the particle density n this gives

$$\nu(\delta t) = \pi \sigma^2 \bar{v}_{12} \delta t n. \tag{4.37}$$

This leads to a temperature decay

$$\frac{dT}{dt} \approx \frac{1}{\delta t} \frac{1}{2} (v_{12}'^2 - v_{12}^2) \nu(\delta t) \approx -n\sigma^2 (1 - \epsilon^2) T^{3/2} \tag{4.38}$$

For viscoelastic particles ϵ depends on T and substituting this back changes Equation (4.38) in the high temperature regime.

From Barker and Henderson [1976] we know heuristic two and three dimensional fits to $g(d)$. Following Ulrich et al. [2009a] we first consider the three dimensional

$$g(d) = \frac{2 - \phi}{2(1 - \phi)^3} \tag{4.39}$$

Putting this all into Equation (4.35) we obtain

$$\frac{dT}{dt} \overset{(4.34)(4.35)(4.36)(4.39)}{=} -\frac{2}{3} \frac{2 - \phi}{2(1 - \phi)^3} d^2 \pi \frac{N}{V} \sqrt{\frac{T}{\pi m}} \tag{4.40}$$

In the case of hard-sphere fluids $g(d)$ is related to the contact value χ

$$\chi \doteq g(2R) \tag{4.41}$$

which is related to the equation of state

$$pV = N k_B T (1 + 4\phi\chi(\phi)) \tag{4.42}$$

Ulrich et al. [2009a] choose the common Carnahan and Starling approximation (see Carnahan and Starling [1969] and Song et al. [1989] why this is a good approximation) following Brilliantov and Pöschel [2004]

$$\chi(\phi) = \frac{1 + \frac{\phi}{2}}{(1-\phi)^3} \tag{4.43}$$

The pair correlation function of the thin thread model should, intuitively, possess two limiting cases: For high energies the energy loss due to bridge ruptures is not significant (it aligns velocities and leads to correlations, but there is nearly no clustering) but for low energies it resembles the sticky gas limit [Yuste and Santos, 1993].

We thus expect two different regimes for high and low temperature. if the temperature is high and therefore the velocity, the probability of bond breaking is $P_{bb} = 1$ and $g(d)$ as well as f_{coll} do not have to be corrected for density effects of clustering. The temperature then follows Haff's law

$$\frac{dT}{dt} \overset{(4.40),(4.45)}{=} T_0 \left(1 - \frac{t}{t_0}\right)^2 [t < t_0] \tag{4.44}$$

where t_0 is given by

$$t_0 \doteq \frac{2\sqrt{\pi m T_0}}{2g(d)\sigma n \Delta E} \tag{4.45}$$

This fails to describe the regime for later times. Ulrich et al. [2009a] propose to correct the equation by looking at the bridge rupture probability P_{bb} We will briefly follow their argument: P_{bb} depends on the fact that the energy is smaller then the bridge rupture energy ΔE, in the limit of $N \to \infty, E \to \infty$ the distribution function of the kinetic energy is Maxwellian

$$w(v) = \left(\frac{m}{2\pi T(t)}\right)^{3/2} \exp\left(-\frac{mv^2}{2T(t)}\right) \tag{4.46}$$

and bridges rupture if the (radial) kinetic energy is smaller than the bridge rupture energy

$$P_{bb} \overset{(4.46)}{=} \int [mv^2/2 < \Delta E] w(v)\, dv \tag{4.47}$$

Evaluating the integral in the asymptotic limit yields in terms of a proportionality constant ν

$$\frac{T(t)}{\Delta E} \propto \frac{1}{\ln \nu t}. \tag{4.48}$$

To augment his findings we propose some corrections for small number of particles

(a) we can compute P_{bb} depending on the center of mass energy of two particles

(b) we know the center of mass distribution function from the one particle energy distribution function

(c) this in turn resembles a Maxwellian for $N > 5$ particles but has to be corrected for the effect of periodic boundary conditions (non-conservation of angular momentum leads to N-1 particles , different energy distribution)

Changing the Energy Distribution Let us reconsider the bridge rupture probability in Equation (4.47). For the first correction we only augment the equation by using the velocity distribution for small N with periodic boundaries from Table 3.1

$$P_{bb} = \int [mv^2 < \Delta E] \frac{\Gamma(D(N-1)/2)}{\Gamma(D(N-2)/2)(2\pi\sqrt{\frac{N}{N-1}})^{d/2}} \left(1 - \frac{N-1}{N}\mathbf{v}^2\right)^{[D(N-2)/2]-1} [E > \frac{N}{2(N-1)}\mathbf{v}^2]\, dv \tag{4.49}$$

we obtain with the help of Gradshteyn and Ryzhik [1980]

$$P_{bb} = \frac{\Gamma(D(N-1)/2)}{\Gamma(D(N-2)/2)(2\pi\sqrt{\frac{N}{N-1}})^{d/2}} \sqrt{8}\sqrt{\Delta E} \;\; {}_2F_1\left(\frac{1}{2}, 1 + D - \frac{DN}{2}, \frac{3}{2}, \frac{\Delta E(N-1)}{EN}\right). \tag{4.50}$$

Here, ${}_2F_1$ is the Hypergeometric function defined by ${}_2F_1(a,b;c;z) = \sum_{k=0}^{\infty}(a)_k(b)_k/(c)_k\, z^k \Big/ k!$

Correction for Clustering In Equation (4.32) we showed how to compute the clustering probability. This is more accurate than Equation (4.47) in the limit of low energies, especially if the critical energy becomes comparable to the system's energy.

Corrections to the Collision Frequency The collision frequency of a particle depends on the average velocity, according to Equation (4.36). With the average relative velocity from Equation (3.19) for $k = 1$ we obtain

$$f_{coll} = g_2(d)\sigma n\langle v_{rel}\rangle \overset{(3.19)}{=} g_2(d)\sigma n \frac{\Gamma((D+1)/2)\Gamma(D(N-1)/2)}{\Gamma(D/2)\Gamma((D(N-1)+1)/2)} \left(\frac{4NE}{N-1}\right)^{1/2} \tag{4.51}$$

Naturally, this proposals have to tested. For the need of such corrections we refer to Kleider [2012] who performed Event Driven Molecular Dynamics Simulations of freely cooling wet granulates and obtained in 2-dimensions a visible difference in the cooling in contrast to the 3-dimensional simulations of Ulrich et al. [2009b]. We add that such corrections are—although in real gases the number of particles is large—important especially if the gas is inhomogeneous or shows clustering in some parts. In this partially clustered areas corrections for small number of particles can become apparent even (as can be seen, e.g., in Figure 3.1) most small-number-effects play only a role for less than 10 disks.

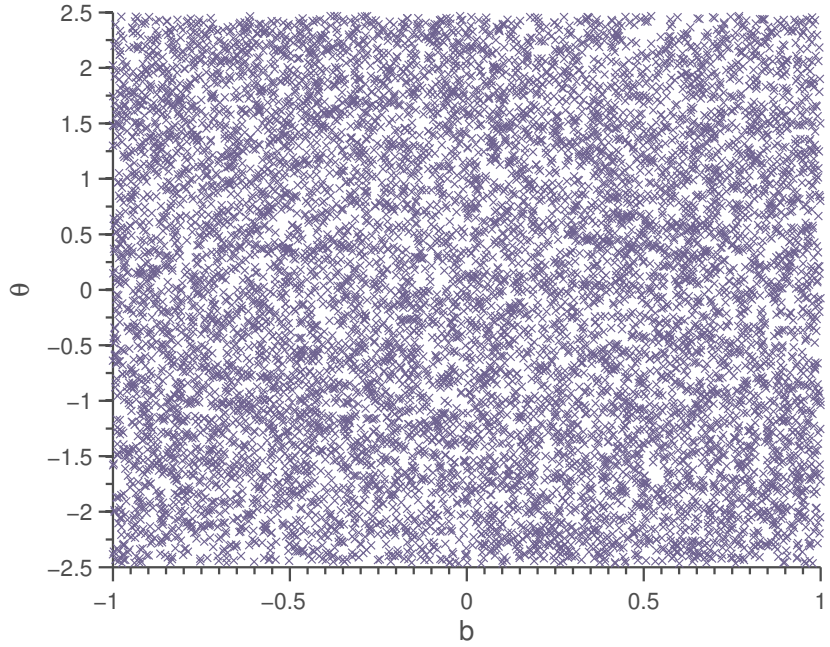

Figure 4.1 – The phase space after 10^3 collision of isoenergetic system. Shown is the two particle system yet the three particle system looks the same if the two particles in whose center of mass frame the coordinates are calculates are chosen at random. It looks as if the natural distribution is uniform. However we note that we only used 10^4 initial conditions. Testing by looking at the cumulative distribution or with the help of a χ^2 tests yields the answer that the phase space is uniform. Glassmeier [2010] resolved a subtle fractal structure inside the phase space; we do not see this with our resolution (which is for long enough times and lots of systems exceedingly demanding for MD simulations).

4.3 Simulation

4.3.1 Ergodicity of the Wet Granular Gas

To discuss the ergodicity of the wet granular gas we first look at its natural distribution. The Sinai billiard is a mixing, symplectic system. Therefore its natural distribution is a uniform distribution and its natural measure is the Lebesgue measure.

The wet granular system is dissipative and it is not obvious what form the natural measure has. Glassmeier [2010] observed a natural distribution with respect to a conditional Lebesgue measure. The condition here was a simple restriction of the measure to the energy shell.

Finding the natural measure with Molecular Dynamics to a high accuracy is non-trivial. The simulations have to run a long time with sufficient many different initial conditions. We use 10^4 different runs. It is questionable if we can resolve the fine fractal structure observed by Glassmeier [2010] that is due to the non-injectivity of the bridge-ruptures. And indeed, in Figure 4.1 we observe no structure in the phase-space. Testing if this distribution is uniform can be achieved by using a χ^2 test or comparing the projections

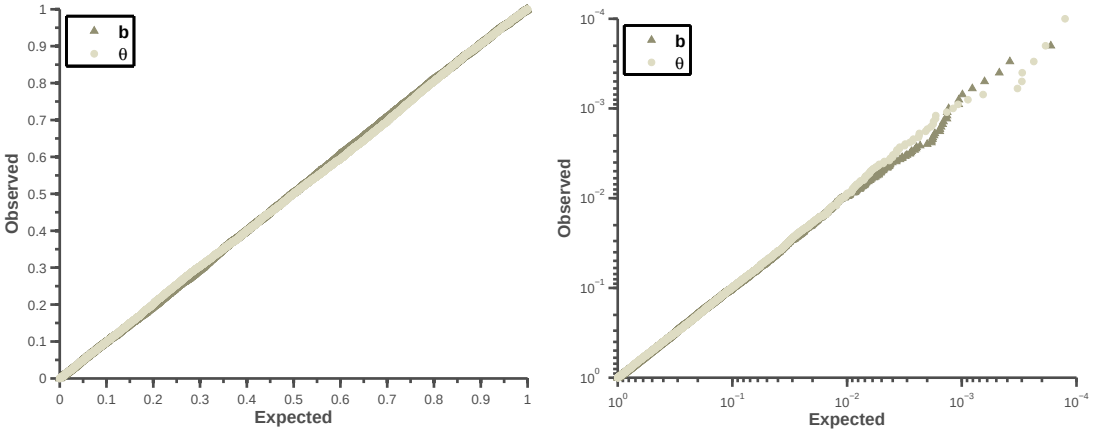

(a) In the quantile/quantile plot of the observed versus the expected—uniform—distribution there are almost no deviations visible. Both the distributions for b, θ lie nicely on the diagonal which corresponds to a good fit between expected and observed distribution.

(b) In the double logarithmic quantile/quantile plot of the observed versus the expected—uniform—distribution there are small deviations visible in the tails. However, these are only pronounced for θ and b smaller than 10^{-3} and can be considered artifacts of the finite statistics.

Figure 4.2 – To test the uniformity of the phase space the distributions of b, θ are compared to uniform distributions. Except for small deviations in the tails the phase space is indeed uniformly distributed.

on the b and θ axis. Glassmeier [2010] notes that both b and θ are uniformly distributed in the wet system, however, comparing with the cumulative distribution function is sometimes problematic and it is not the most robust test of uniformity available. To see this a quantile-quantile plot is used in Figure 4.2a that corresponds to comparing the cumulative distribution function to a line-segment. The deviations are minute, however in Figure 4.2b it becomes apparent that the uniformity is somehow mitigated in the tails of the distribution.

4.3.2 Free Cooling

The uniformity of the natural distribution allows us to propose that no structure from the two disk interaction remains in the many-body simulations. We extend the study of two disk free cooling for different particle numbers and compare the results to Glassmeier [2010].

If the same parameters (initial Energy, rupture length, bridge rupture Energy) are used we expect a good agreement between the billiard and Molecular Dynamics simulations. We start by considering free cooling. We simulate 10^3 system's of different number of disks (2–10) with uniformly distributed initial positions and velocities. We additionally remove the center of mass motion and initialize our simulations such that center of mass lies in the middle of the system The initial energy is also distributed uniformly for $N > 3$ (The removal of center of mass motion results in a fixed initial energy distribution of

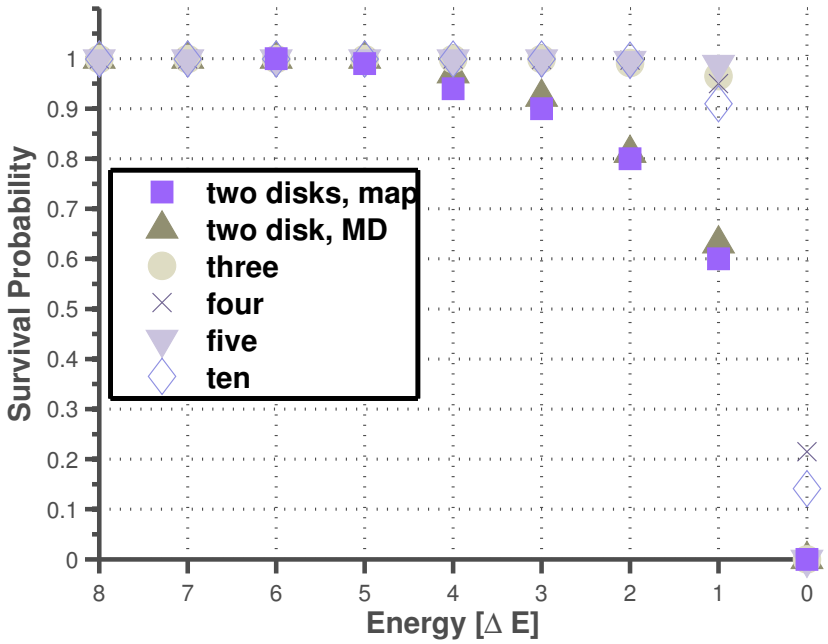

Figure 4.3 – Shown is the survival probability of a system of N disks with initial energy of 10^4 distributed uniformly (for N>2 disks). The survival probability denotes the number of system that still loose energy (which is only possible if the system is not clustered) to the number of clustered systems. In the two disk case this clustering for higher than zero energies can be understood as the two particles circling one another. For two particles the Molecular Dynamics simulations fit the systems studied by Glassmeier [2010]. For higher number of disks the survivability curve drops of steeper. This can be attributed to the possibility of a third particle colliding with two bound particles and thus freeing them. Hence in the limit of $N \to \infty$ the probability that all of the system is clustered should drop of like a Heaviside function. This can be seen in e.g. large scale Event Driven Molecular Dynamics simulation where even after some time particles still move freely although most of the system has already clustered.

the two disk simulations). The simulations were carried out with a time-step $\Delta t = 10^{-5}$ for 10^9 iteration steps thus allowing us to simulate up to a time of $T = 10^4$.

For two particles the simulations match nicely with Glassmeier [2010]. As can be seen in Figure 4.3 the two-disk system shows the same cooling behavior. For more than two particles the curves align more and more to a steep fall. This is in line with Equation (4.28) and the reasoning that it becomes more and more unlikely for the whole system to cluster if the number of particles increases.

The clustering probability depends on the relative energy distribution and this in turn on the one-particle energy distribution. In the case of two particles this distribution is simply a Delta-distribution since the center-of-mass motion is removed. For more then two particles the distribution follows the constrained Maxwellian distribution from Table 3.1 in the high energy limit.

For energies that are large in comparison to the bridge rupture and critical energy the theories match nicely as can be seen by comparing their cumulative distribution function, see Figure 4.4 . For low energies the disks can form clusters if the energy

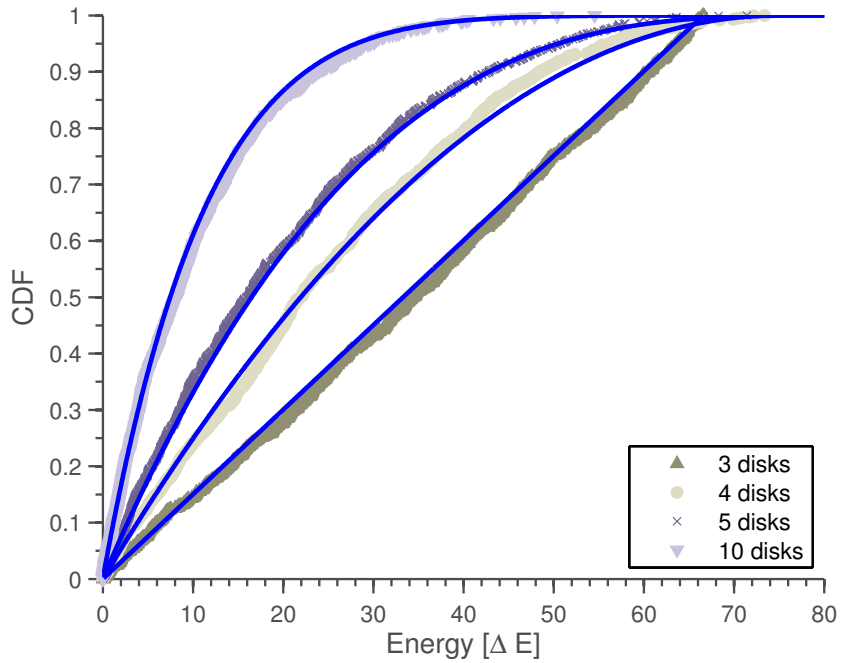

Figure 4.4 – The one particle energy distribution function for the elastic gas is Maxwellian. With periodic boundary conditions the additional constraint that the center of mass velocity is conserved reduce the degrees of freedom. Thus instead of the N-particle distribution function we expect the elastic gas to follow the $N-1$ distribution. We checked this for different number of particles that were initialized with uniform energy distribution of $E_0 = 10^4$ after $9.99 \cdot 10^4$ collisions for 10^4 systems with remaining energy $E = 100$. We compare the cumulative density function. The simulations fit neatly. The comparison above was made for an inelastic system with the energy conditioned by $E(n) = E_0 - n\Delta E$. It shows that the deviations in the energy distribution are small if the average energy is high enough, $\Delta E \gg \Delta E$

is near the critical energy. This and the correlations induced by the higher likelihood of two-particle pairs lead to deviations in the energy distribution. The extent of this deviations are non-negligible: see Figure 4.5.

Correlation Function Another, interesting, insight can be gained by considering the velocity auto correlation function.
The velocity auto correlation function is defined by

$$C_i(t) \doteq \langle v_i(t) v_i(t) \rangle \tag{4.52}$$

For long it was expected that the velocity auto correlation function decays exponentially. However, even for hard-sphere systems this is no longer true. Alder and Wainwright [1970] discovered that the velocity auto correlation function decays algebraically. Chernov and Markarian [2003] showed that in the finite horizon billiard that the decay should be exponential. For hard-sphere and granular gases in D-dimensions the veloc-

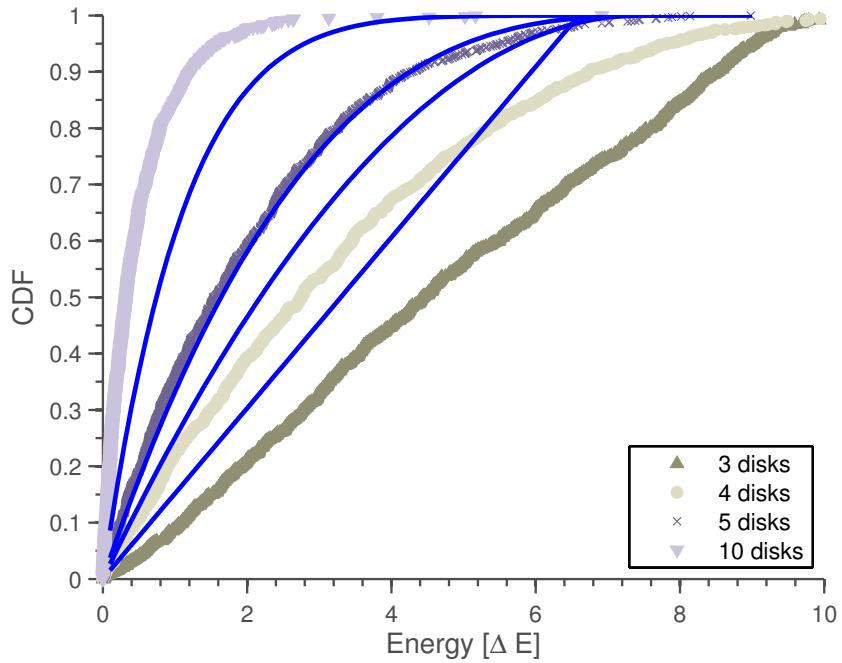

Figure 4.5 – In the limit of low energies we expect deviations from the hard-sphere behavior and the energy distribution from Table 3.1. For $E = 10$ the deviations are clearly visible since from an energy of $E_{crit} \approx 6$ disks can cluster.

ity auto correlation function scales like

$$\approx t^{-\frac{D}{2}} \tag{4.53}$$

We obtain the exponents of the velocity auto correlation function by a linear fit to a double logarithmic plot; in principle the maximum likelihood fit yields more correct estimates. However, due to the large sample size this discrepancy can be neglected. Our simulations confirm an algebraic decay with t^{-1} as can be seen in Figure 4.6 with numerical data in Table 4.1.
We additionally checked that the correlation function decays with the same exponent in the sheared two and three body system. Figures for this can be found in the Appendix A.

Number of disks	Fitted Exponent	Error
2	-0.955	0.12
3	-0.964	0.11
4	-0.954	0.11
5	-0.953	0.14
10	-0.96	0.12

Table 4.1 – The velocity auto correlation function decays algebraically with an exponent of -1. This exponent is of negligible variance for different number of particles. The error here, is one standard deviation obtained by a standard linear fit, checked with Gnuplot.

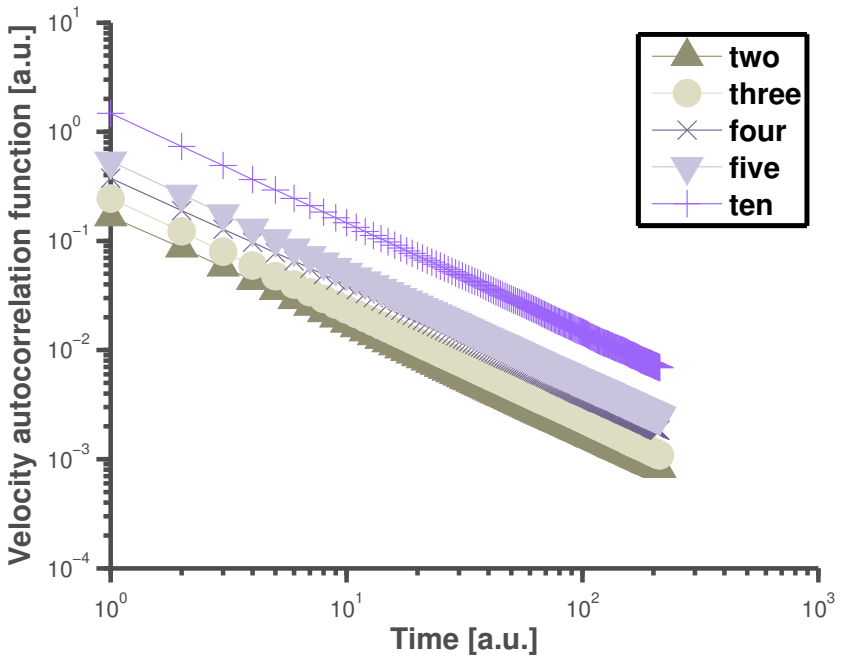

Figure 4.6 – The velocity auto correlation function for systems with different number of disks over time. The velocity autocorrelation function decays algebraically with t^{-1}. This is expected for hard-sphere systems. In this plot the disks were initialized with an energy 10^4 in units of bridge rupture energy.

Chapter 5

Sheared Systems

We derive a stochastic description for the energy distribution of the sheared system. We show how a scaling ansatz for the lifetime distribution can be obtained. Comparing this with the simulations we note that the average energy of the systems that are not already clustered increases. However, the clustered state is still absorbing: for all shear rates the systems will eventually cluster. We then allude that this absorbing state is not a two particle peculiarity but persists for many particles. The main difference is that the lifetime becomes very long since the probability of the whole system to cluster becomes smaller as was noted for the freely cooling system.

5.1 Theory

We use Lees Edwards boundary conditions to inject energy. The amount of energy injected depends on how often the particles cross one of the sheared boundaries compared to how often they collide. We call ν the average number of Lees Edwards crossings per collision

In a sheared system the ensemble average of the energy change per collision is

$$\delta E = \nu \frac{s^2}{2} - \Delta E. \tag{5.1}$$

Hence, the expected value for the system's net energy increases if

$$\delta E > 0. \tag{5.2}$$

This is possible for a critical shear rate $\mathfrak{s}$ that is obtained by comparing Equation (5.1) and

$$\mathfrak{s} \overset{(5.1),(5.1)}{=} \sqrt{\frac{2\Delta E}{\nu}} \tag{5.3}$$

We assumed that ν is constant in time. This is not obvious since for systems with, e.g., N =3–10 disks two particles may be clustered and are thus highly correlated. This probability in turn depends on the energy which depends on time.
The processes responsible for the change in energy are the crossing of Lees Edwards boundaries and the rupture of liquid bridges. For the Lees Edwards boundary crossing we define the operator $\mathfrak{L}$ to be

$$\mathfrak{L}\mathbf{v} \doteq \sqrt{\mathbf{v}^2 + \mathbf{s}^2 + \mathbf{vs})} \tag{5.4}$$

and the bridge rupture operator $\mathfrak{B}$ to act like

$$\mathfrak{B}v \doteq \sqrt{v^2 - 2\Delta E} \tag{5.5}$$

For the following, assume that b and θ are uncorrelated, this is only justified if the correlations decay fast. Since the Sinai billiard is hyperbolic, the natural distribution is uniform and if we restrain the analysis to energies larger than the critical energy this approximation should yield good results.
Since the system is not directly effected by any dependence on b this may be averaged out and since b is uniformly distributed we get rid of this coordinate.
However, what is correlated are the boundary crossings and θ. According to Glassmeier [2010]

$$P(\text{crossing}|\theta) = \begin{cases} \frac{L}{2}\|\sin\theta\| & \text{if } \|\sin\theta\| < \frac{2}{L} \\ 1 & \text{if } \|\sin\theta\| \geq \frac{2}{L} \end{cases} \tag{5.6}$$

Clustering is actually an additional stochastic process that has to be considered. The approximation of a constant cluster probability C however gives a good approximation. This resembles a probability-density function $P(\text{cluster}|v)$ that is 1 if $v < C$ and zero otherwise. The constant C must fulfill

$$P(cluster) = \int_0^{\sqrt{2E_c}} P(\text{cluster}|v_{\text{rel}})P(v_{\text{rel}})dv_{\text{rel}} \overset{!}{=} \int_0^C P(v_{rel})dv. \tag{5.7}$$

where $P(\text{cluster}|v_{rel})$ is $P(\text{cl}|E_{rel})$ from Equation (4.12) by changing $v_{rel} = 1/2E_{rel}^2$.
Glassmeier [2010] notes that obtaining $P(v_{rel})$ is difficult because the dominating contribution in Equation (5.7) results from small energies. With the large deviations from Figure 4.5 in mind, together with that the sheared systems also show a energy distribution further complicates the matter.

Nonetheless we can choose a $C > \sqrt{2\Delta E}$. Glassmeier [2010] chooses

$$C = \sqrt{3} \tag{5.8}$$

and obtained good results.
With this we formulate the problem as a random walk with absorbing boundary for $E < C$ (at least in the two particle case).
We do this the following way

$$v_{n+1} = \begin{cases} \mathfrak{B}^X \mathfrak{L} v_n & v_n > C \\ 0 & v_n < C \end{cases} \tag{5.9}$$

where X is a random variable that is uniformly distributed between 0 and v. Notice, that we neglected the correlations of $P(\text{crossing}|\theta)$
It is surprising that this simple dynamic results in an exponential distribution of energies without the θ correlations and qualitatively right deviations with correlations. Glassmeier [2010] also proposes that one can exchange the order of bridge rupture and collision - however since $[\mathfrak{B}, \mathfrak{L}] \neq 0$ one also has to adapt the constant C in a non-obvious way.

5.2 Fokker-Planck Description

The stochastic model describes a simple Master Equation or generalized random walk. This leads to a Fokker-Planck description of the probability density function.
A Fokker-Planck equation describes the evolution of a probability density $P(v,t)$ in terms of drift, proportional to the drift coefficient $M(x)$, and diffusion, proportional to the diffusion constant $D(x)$. In this chapter the dimension of the system will be set to 2 and with D we will only refer to the diffusion coefficient. The Fokker-Planck equation is defined as

$$\partial_t P(v,t) = -\partial_v (M(v)P(v,t)) + D/2\partial_v^2 P(v,t). \tag{5.10}$$

Intuitively, the model from describes a random walk in absolute-velocity space. The drift and diffusion coefficients depend on the change of velocity (if we use velocity as our prime variable) according to

$$\begin{array}{lll} M \doteq \langle(\Delta v)\rangle & = \int (\Delta v) P_\theta(\theta|v_n) d\theta & = \frac{1}{\pi}\int_0^\pi (\Delta v) d\theta \\ D \doteq \langle(\Delta v)^2\rangle & = \int (\Delta v)^2 P_\theta(\theta|v_n) d\theta & = \frac{1}{\pi}\int_0^\pi (\Delta v)^2 d\theta \end{array} \tag{5.11}$$

the velocity difference between two time-steps is given by Equation (5.5).

$$\Delta v \doteq v_{n+1} - v_n = \sqrt{v_n^2 - 2\Delta E + \langle X\rangle(s^2 + 2sv_n\cos\theta)} - v_n \tag{5.12}$$

Glassmeier [2010] approximates Δv in a series expansion to first order, noting that clustering can - in any case - not be modeled with this simple approach. Her approximation reads

$$\Delta v = -\frac{\Delta E}{v} + \frac{\langle X \rangle s^2}{2v} + s\langle X \rangle \cos\theta - \frac{\langle X \rangle^2 s^2 \cos^2\theta}{2v} + \mathcal{O}\left(\frac{1}{v^2}\right) \tag{5.13}$$

From this one can calculate the drift and diffusion easily

$$M \overset{(5.11),(5.12)}{=} \frac{\frac{\langle X \rangle}{2} s^2 - \frac{\langle X \rangle^2}{4} s^2 - \delta E}{v} \tag{5.14}$$

$$D \overset{(5.11),(5.12)}{=} \frac{\langle X \rangle^2}{2} s^2 \tag{5.15}$$

Note that the diffusion coefficient does not depend on energy directly. However, if formulated for the energy instead of the velocity Glassmeier [2010] obtained

$$M_E = \frac{\langle X \rangle^2}{2} s^2 - \delta E \tag{5.16}$$

$$D_E = \left(\frac{\langle X \rangle}{2} s^2 - \Delta E\right)^2 + \frac{\langle X \rangle^2 s^2}{2} E \approx E \tag{5.17}$$

In the limit $v > s$ one can neglect the drift. Without drift the Fokker-Planck equation for $P_{E_0}(E)$ can be understood as a simple diffusion equation for which the solution is the well known decaying gaussian. For us, the scaling-behavior of $P_{E_0}(E)$ is more important than the exact solution. The diffusion ansatz, made by Glassmeier [2010], uses

$$\frac{E}{\langle E \rangle} = \frac{v^2}{2kDt}. \tag{5.18}$$

Also—because of the absorbing boundary for $v < C$—the clustering is assumed to behave like a Poisson process for which the percentage of clustered states is given by

$$n(t) \approx t^{-\gamma} \tag{5.19}$$

Glassmeier [2010] also concludes that a relation for survival exponent γ can be found such that it respects $\gamma \propto s^{-2}$. In the next section we will see if our simulations can confirm this finding and if this behavior persists for more than two disks.

5.3 Sheared Simulations

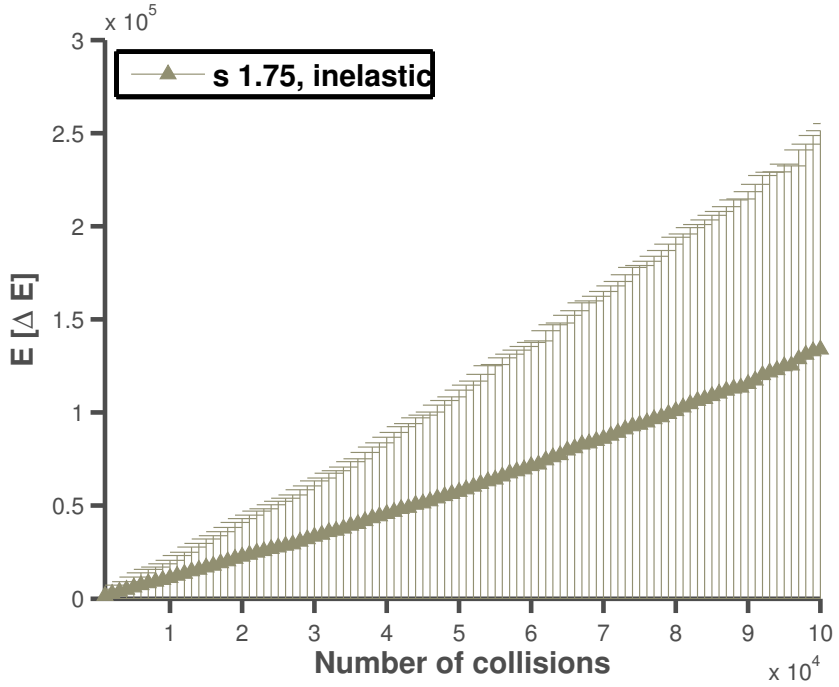

Figure 5.1 – Shown is the increase in energy of a system initialized with uniform one particle energy distribution for three disks. The initial energy is 10^4 and the system is sheared with $s = 1.75$. The starting conditions are: uniform distribution in position and velocity with the center of mass velocity removed. The plot shows the increase in energy in units of bridge rupture energy over time measured in number of collisions. Also the standard deviation of the average energy was added to the plot. Although the ensemble used consists of 10^3 systems the standard deviation grows and always encompasses zero energy. This corresponds to a finite probability of a system with high energy to end up in a clustered state which renders the system only transient. In this sense the three disk system resembles the two disk iterated map studied by Glassmeier [2010]

5.3.1 Heating

Adding shear to the system injects energy proportional to the shear rate s.
Let us first study the increase in energy for different number of particles and different shear rates. From Equation (2.52), we expect the energy to increase with s^2 on average if the bridge rupture energy can be neglected. For a range of systems with different shear rates for three and two disks respectively we obtain the average energy increases found in Figure 5.2 and Figure 5.3. We expect an asymptotically linear increase with time according to Equation (2.52) and indeed this is the case.
A detailed account for the shearing rate of $s = 1.75$ with error bars can be found in Figure 5.1. Noticeably, the standard deviation of the energy increases with time and always encompasses the clustered state in one sigma. This means even for an increase of average energy there is still a probability that a system ends up in a clustered state.

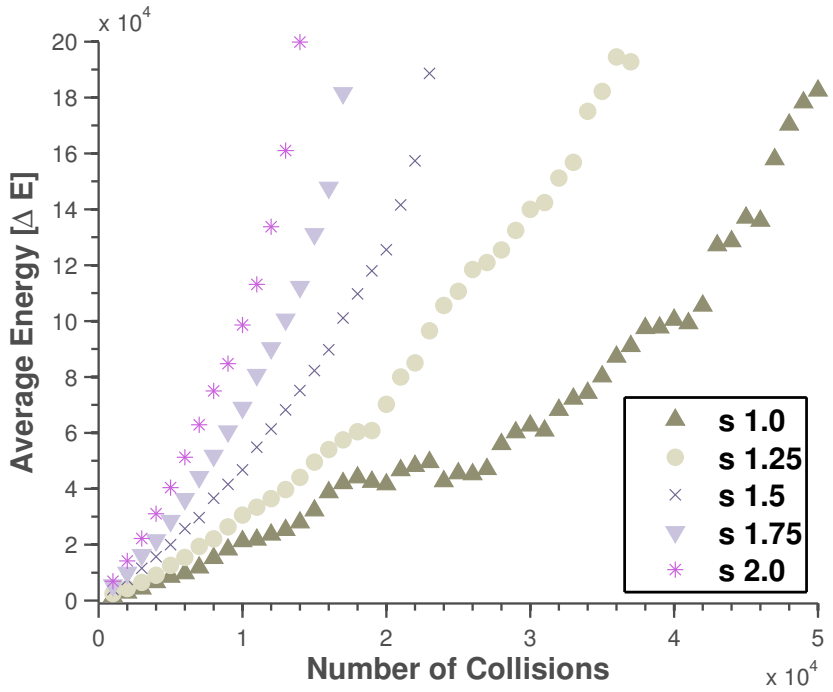

Figure 5.2 – Shown is the increase in average energy of the two disk system for different shear rates. Since the clustered systems are not averaged over the energy increases for all shear rates. Asymptotically the increase in energy is linear.

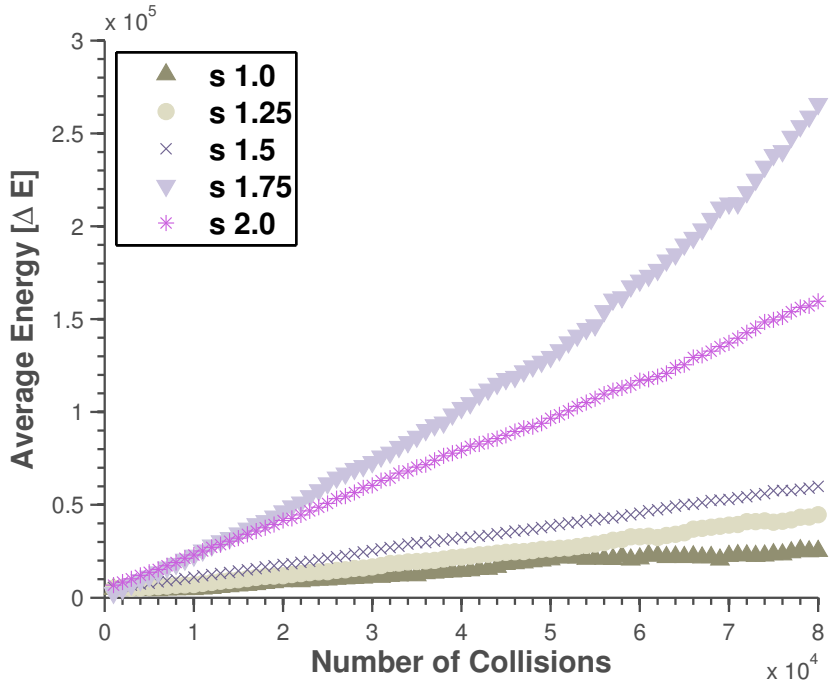

Figure 5.3 – Shown is the increase in average energy of the three disk system for different shear rates. Since the clustered systems are not averaged over the energy increases for all shear rates.

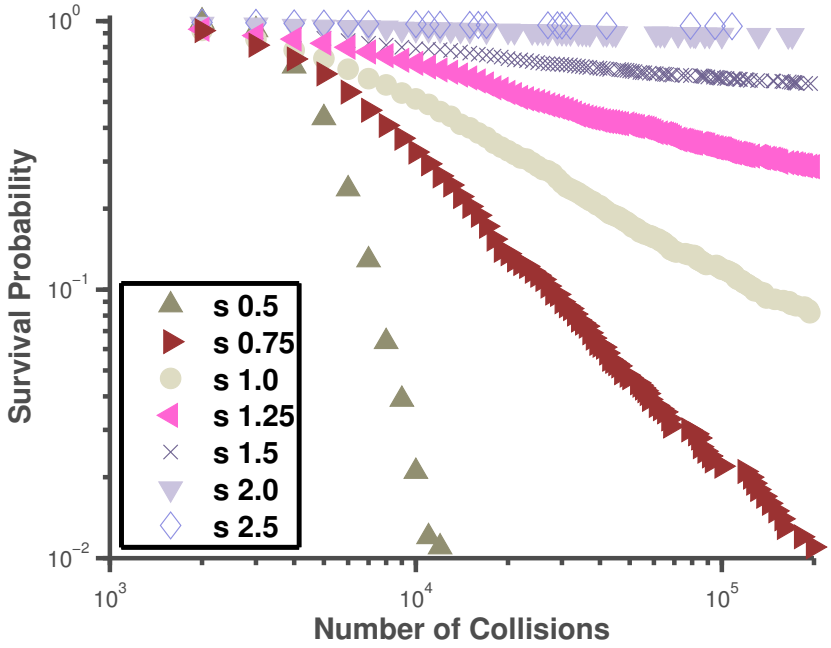

Figure 5.4 – If one looks at the survival probability of the sheared two disk system it becomes apparent that there still exists an absorbing state in form of a clustered system. This is surprising because the system is heated by injecting energy via the Lees Edwards boundaries with $\approx s^2$ per number of collision and for approximately 2 boundary crossings per collision the average gain in energy compared to the loss $2s^2 > 1$ should lead to a increasing overall energy for high shear rates. This is not the case since there is still a non-zero clustering probability for systems with $s > 1.5$.

5.3.2 Clustering

Counter-intuitively not only the average energy increases but also the standard deviation of the one-system energy. This standard deviation always encompasses zero energy in one sigma. This means that, although we have an average increase of energy, the transient state of a clustered system persists. To study this we look at the survival probability of the sheared billiard. We do this for 2, to compare to the simulations of Glassmeier [2010], and 3 to study if this is a two-particle phenomena or system inherent. For two particles we indeed find a persisting leak conformant with Glassmeier [2010] in Figure 5.4. For three disks we find that this still exists again even for systems where the average energy increases. However, in the three particle case the lifetime distribution decays more slowly for high enough shear rates. The reason for this can be found in that—as is the case for the clustering in free cooling—the probability for a whole system of N particles to cluster completely whilst having more energy than the bridge rupture energy decreases with the number of particles.
To confirm the scaling ansatz of Glassmeier [2010] we fit the survival exponents in Figure 5.6.
We can see that the exponent of the survival probability indeed decays with the shear

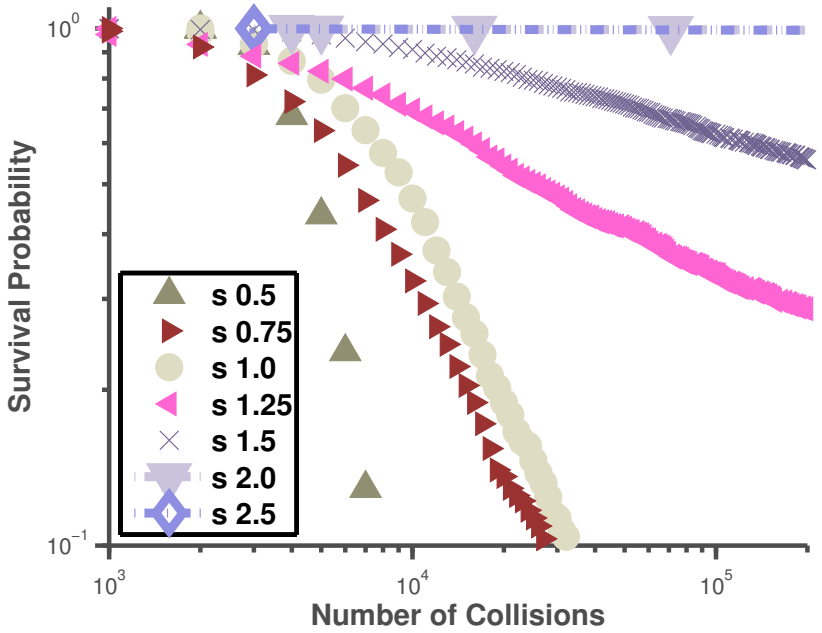

Figure 5.5 – For three disks the leak still exists but the probability for the whole system to cluster is smaller (note that the initial energy is still the same as in the two particle case, thus the energy per particle is smaller and for low energy-injection the system clusters faster). We find a critical shear speed over which there is nearly no clustering. This is not surprising because on each boundary crossing the energy added into the system transceeds the bridge rupture energy.

rate. The plot also confirms the scaling proposed by Glassmeier [2010] of $\gamma \propto 1/s^2$. It is also visible that at first the three disk system shows shorter lifetimes. We remark that this is also due to the effect that we initialized the systems isoenergetically with $E = 10^4$ and thus more energy is shared between the disks in the three-disk system.

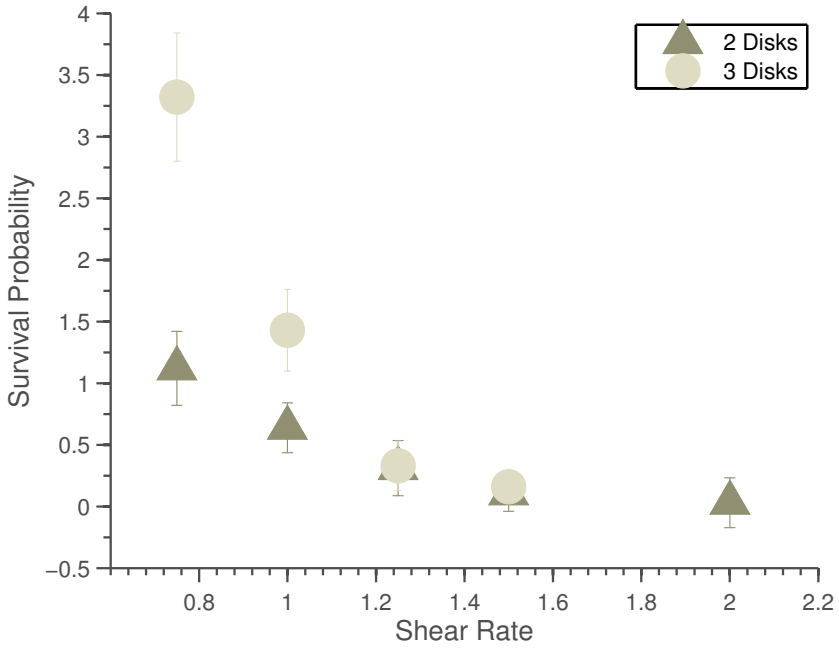

Figure 5.6 – Survival exponents for the two and three disk system. With higher shear rate the exponent decreases until it converges to zero for high energies. As Glassmeier [2010] proposed the survival exponent scales according to $\gamma \propto 1/s^2$. In both cases the exponent decays to zero which means, that for high enough shear rates a clustering is still possbile, however, it will take much longer.

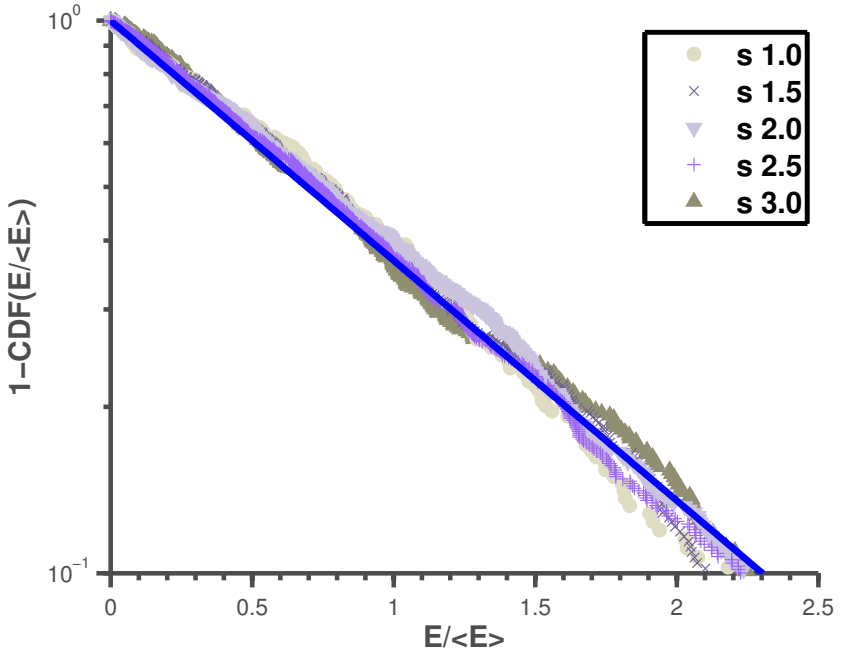

Figure 5.7 – Ensemble energy distribution of sheared two particle system. The evolution of the energy distribution can be understood as governed by a generalized random walk in energy space with an absorbing boundary if the energy decreases below the bridge rupture energy. Since it can be modeled by a Fokker-Placnk equation the energy shows an exponential shearing. This is confirmed by the numerical data.

5.3.3 Energy Distributions

To understand this clustering we further investigate the ensemble energy distribution. The ensemble one can be found in Figure 5.7 for two disks and in Figure 5.8 for three disks. In Equation (5.18) the scaling form for the energy distribution is shown. Since the exponential distribution $P(E)$ follows is "broad" and indeed the standard deviation grows in the diffusion process, as was confirmed for the average energy increase and its standard deviation. For three particles we, additionally, have a one particle energy distribution function that is not a Delta distribution. However, it still looks the same: The energy is distributed uniformly as has been shown in the free-cooling Chapter and thus the one particle energy distribution should not look different from the ensemble distribution as it is a function of the exponential distribution.

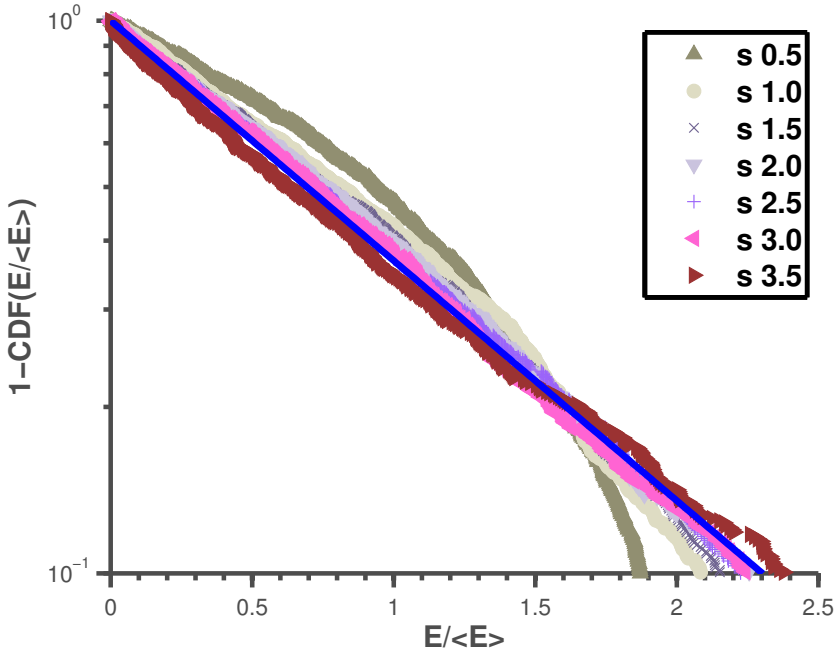

Figure 5.8 – Ensemble energy distribution of sheared three particle system. The evolution of the energy distribution can be understood as governed by a generalized random walk in energy space with an absorbing boundary if the energy decreases below the bridge rupture energy. Since it can be modeled by a Fokker-Placnk equation the energy shows an exponential shearing. This is again confirmed by the numerical data.

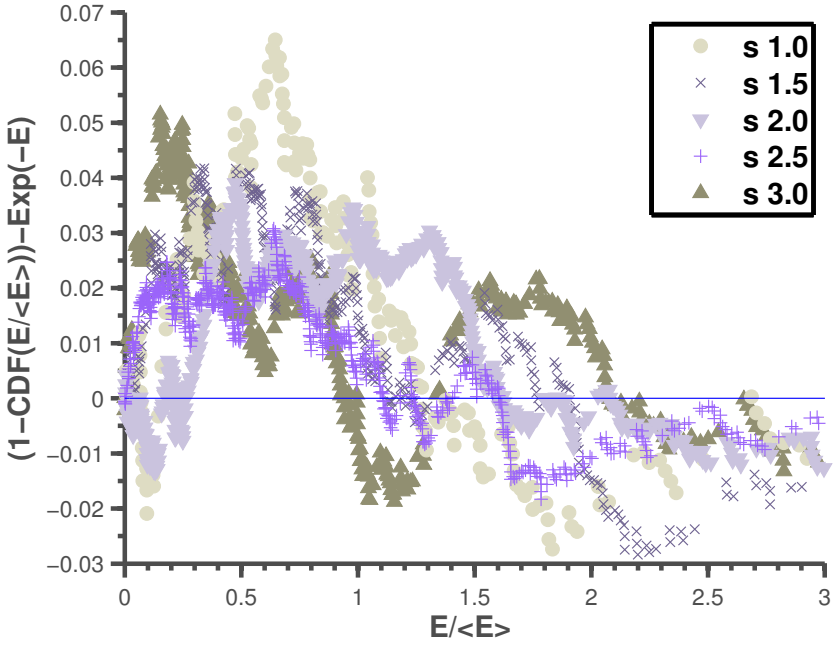

Figure 5.9 – According to the stochastic model the energy distribution of the ensemble, i.e., the probability that an ensemble has a certain energy, behaves exponential. Shown here is the difference of the cumulative distribution function to the exponential distribution (note that $\int_0^\infty \exp(E/\langle E\rangle) = \langle E\rangle(1 - \exp(E/\langle E\rangle)$ and thus we compare it to one minus the cumalite distribution function)). Shown here is the two disk system after 10^4 collisions for different shear speeds. The simulation and the scaling ansatz fit nicely for high shear rates. The approximation becomes better with higher shear rates because for low rates the drift term and the absorbing state dominate.

We also investigate the deviations in of the energy distribution function to the exponential scaling ansatz. This can be found in Figure 5.9 and Figure 5.10. In both cases the deviations depend on the shear rate. In general the scaling ansatz fits more closely for high shear rates. This is not surprising, since for small shearing the absorbing state of a clustered system is much more prominent and the drift dominates the diffusion term in the Fokker-Planck model.

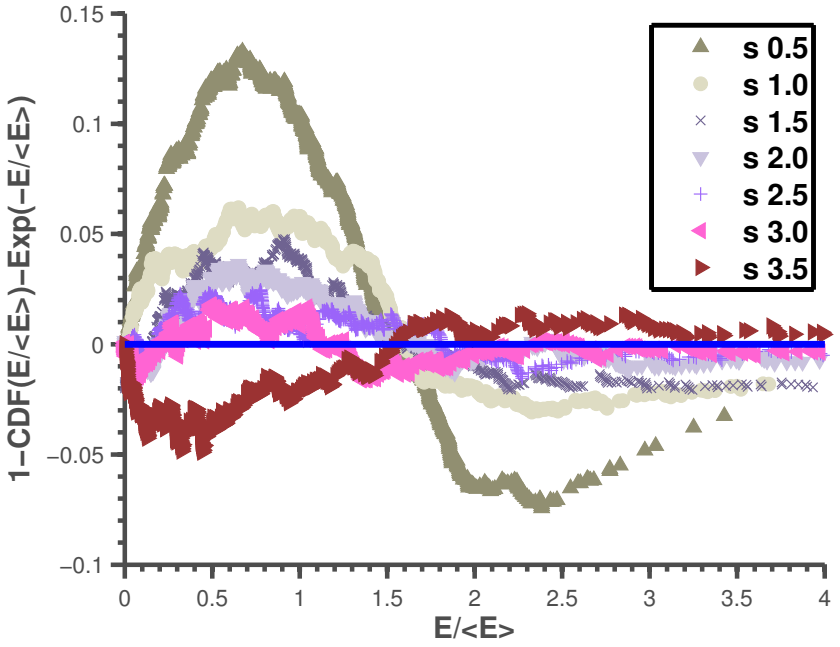

Figure 5.10 – According to the stochastic model the energy distribution of the ensemble, i.e., the probability that an ensemble has a certain energy, behaves exponential. Shown here is the difference of the cumulative distribution function to the exponential distribution (note that $\int_0^\infty \exp(E/\langle E\rangle) = \langle E\rangle(1 - \exp(E/\langle E\rangle)$ and thus we compare it to one minus the cumalite distribution function)). Shown here is the three disk system after 10^4 collisions for different shear speeds. The simulation and the scaling ansatz fit nicely for high shear rates. The approximation becomes better with higher shear rates because for low rates the drift term and the absorbing state dominate. For $s = 3.5$ the questions of data accuracy occur since the energy after 10^4 collisions is very large and thus numerical problems can arise.

Chapter 6

Summary

The wet billiard provides an excellent model system for the study of non-equilibrium physics. It is strongly chaotic with a natural distribution that is uniform. Yet the freely cooling as well as the sheared system are transiently chaotic: the absorbing state is a clustered system and it exists even when the average energy increases.
The differences of the many-body system to the Sinai billiard can be summarized in the following aspects

The one particle energy distribution appears for $N > 2$ disks. Along with it distributions for the relative momentum and relative energy are introduced. If the system's energy is noticeably larger than the critical energy these distributions match the classical Maxwellian distributions closely.

The clustering for more than two disks is influenced by the addition of the one particle energy distribution. Although it becomes possible to form two-particle clusters in $N > 3$ for arbitrary energies, the clustering of the whole system becomes more unlikely. In the limit of many particles the complete energy has to be dissipated such that no particle can be freed by collisions.

Additionally to this we have proposed

Changes to the collision frequency. We can bridge the small Sinai billiard to "large-scale" observables. This is possible by using the Maxwellian limit as well as the clustering probability from the Sinai billiard.

We also confirmed

The Sinai billiard is strongly chaotic it possesses a natural distribution that is distributed uniformly when projected on the degrees of freedom.

For the sheared systems we confirmed that the

Increasing of average energy—while a leak persists—is not a peculiarity of the two-disk billiard but instead that the average energy of the non-clustered systems increases; and that this general mechanism that carries over to few particles.

We also discussed the

Existence of an absorbing state. The survival probabilities decay algebraically for the two and three billiard system. However, since the probability of the whole system to cluster is lower, the absorbing state is harder to reach the more particles are investigated.

The reason for this can be seen in the fact that

The two and three disk system can be modeled as undertaking a random walk in energy space. This leads to the—succesfull—scaling ansatz for the exponential energy distribution function. Comparing with numerical data for both the two and three disk system confirmed this mechanism.

In summary we showed that we can bridge the gap between the many particle limit and the two particle billiard. There, naturally, remain a great many open questions.

To study the scaling of the energy distribution in the sheared system we will perform simulations for more than 3 disks, since from three disks onwards the one particle energy function is not uniform anymore but tends to the Maxwellian.

In the line of using the Sinai billiard, we can investigate different methods of energy injection. For example by using moving, reflecting boundaries. This would mimic shaking, that is often used to inject energy in laboratory experiments of granulates. Furthermore, the study of billiards with such moving boundaries is part of recent research, regard for example Loskutov et al. [2008]. Since wet granulates have proven to be an interesting model system, the question arises what new phenomena can be studied if the system is used under different energy injection mechanisms.

We can ask how the system's behavior depends on the geometry. This could be altered: it is easy to introduce an anisotropy by adding, e.g., gravity, or discussing different shapes of granulates. Especially with periodic boundary conditions the constrained Maxwell distribution has a non-trivial dependence on masses. Can this be seen if the masses of disks are, e.g., distributed according to a Gaussian distribution?

Another aspect that remains open to investigation is what happens if rotational degrees of freedom are introduced. As alluded in the Introduction there is a non-trivial interplay between rotation and translation. Especially if there is equipartition with respect to both types is under discussion.

All in all, we can see that there is a great many fascinating research to be done in studying wet granulates and small dissipative systems.

Appendix A

Correlation Functions in Sheared Systems

Additionally, we can again look at the correlation functions. The velocity auto correlation function is not influenced by the boundary conditions as can be seen in Figure A.1 for two and Figure A.2 for three disks.

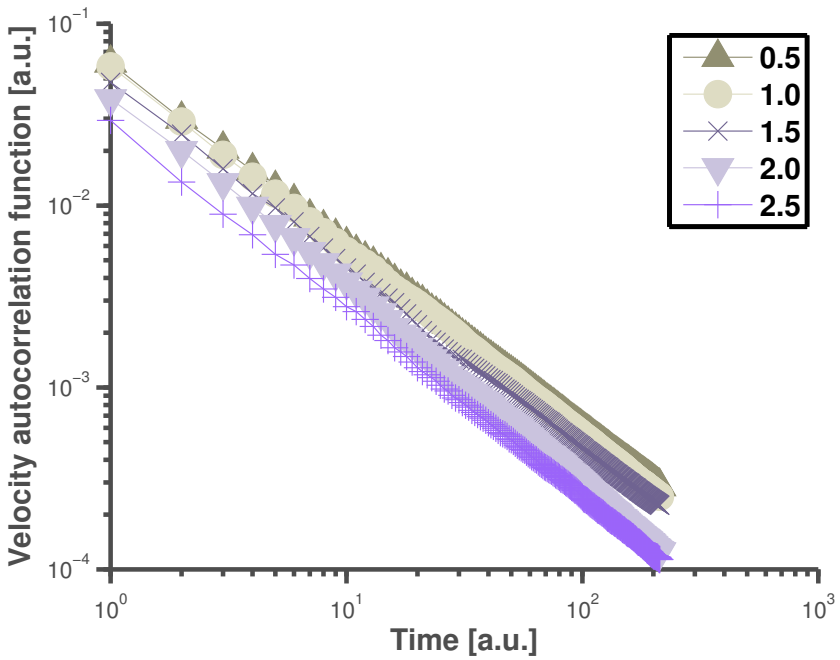

Figure A.1 – The velocity auto correlation function for systems with different shear speeds over time for the two particle system. The velocity autocorrelation function decays algebraically with t^{-1}. This behavior is expected for hard-sphere systems and is interesting to observe that this still holds for sheared systems. In this plot three disks were initialized with an energy 10^4 in units of bridge rupture energy.

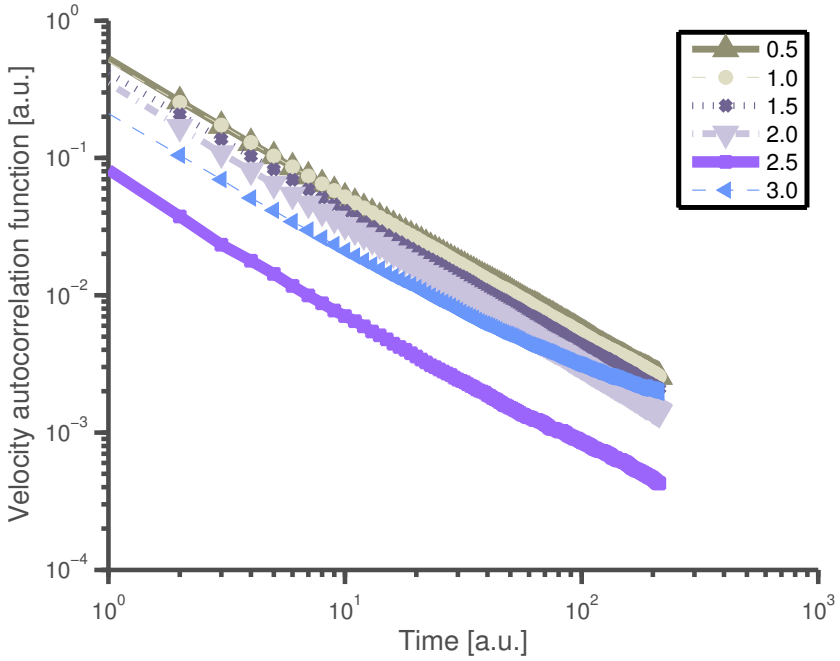

Figure A.2 – The velocity auto correlation function for systems with different shear speeds over time for the three particle system. The velocity autocorrelation function decays algebraically with t^{-1}. This behavior is expected for hard-sphere systems and is interesting to observe that this still holds for sheared systems. In this plot three disks were initialized with an energy 10^4 in units of bridge rupture energy.

Appendix B

Molecular Dynamics Code

B.1 Tests

To validate the simulations we can use the following tests

Initial Condition For a total of 10^5 initial conditions with isoenergetic energy and disk numbers $N = 2, 3, 4, 5$ it was tested if: the energy is uniformly distributed and if the initial conditions are uniformly distributed

Elastic Collisions For two disks with initial coordinates $(-1, 0)$ and $(1, 0)$ and non-zero relative velocity there should be infinitely many elastic collisions without loss of energy. The test passes if, after 10^6 collisions there is no noticeable energy deviation or deviation in y-direction.

Inelastic Collisions For two disks with initial coordinates $(-1, 0)$ and $(1, 0)$ and non-zero relative velocity the particles loose δE in each of their collisions until their relative velocity is below the threshold to rupture the liquid bridge. The initial energy of 10^6 is compared to the energy decrease of 1 per collision if there are no deviations the test passes.

Integrator One disk with initial conditions $(0, 0)$ and initial velocity $(1, 1)$ is simulated for 10^5 time-steps. Since the velocity is known the deviation from the analytic result and the simulation can be compared.

Lees Edwards Boundary Conditions For one disk with initially zero velocity in x-direction but a velocity of 1 in y direction and defined shear rate $s = 2$ the energy, the y-velocity and the offset is compared.

Collisions and Bridges over Lees Edwards Boundary Conditions Two particles are initialized at the position y-position $-ly + 0.5$ and $ly - 0.5$, both with a radius $r = 1$. However, their x position differs such that they are not in contact at $t = 0$. If the system is sheared the particles will collide since they move relative to one another because of the moving reference frames at a defined time. Also, a liquid

bridge will form that attracts the disks to one another and thus leads to a non-zero velocity in x-direction. By making a movie of this, the correctness of this can be easily verified.

Elastic Simulations For 100 disks the simulations are run for 10^4 collisions and the energy distribution is compared to a Maxwellian with a χ^2 test. If the χ^2 test passes, so does the whole test.

Bibliography

Alder, B. J. and T. E. Wainwright. Decay of the Velocity Autocorrelation Function. *Physical Review A*, 1(1):18–21, Jan. 1970.

Aspelmeier, T. *Microscopic models of energy dissipation by internal degrees of freedom in particle collisions*. PhD thesis, Universität Göttingen, 2000.

Ausloos, M., R. Lambiotte, K. Trojan, Z. Koza, and M. Pe¸kala. Granular matter: A wonderful world of clusters in far-from-equilibrium systems. *Physica A: Statistical Mechanics and its Applications*, 357(2):337–349, Nov. 2005.

Barker, J. A. and D. Henderson. What is "liquid"? Understanding the states of matter. *Rev. Mod. Phys.*, 48:587–671, Oct 1976.

Beijeren, H. V. and M. Ernst. The modified Enskog equation. *Physica*, 68(3):437 – 456, 1973.

Ben-Naim, E., B. Machta, and J. Machta. Power-law velocity distributions in granular gases. *Physical review E, Statistical, nonlinear, and soft matter physics*, 72(2 Pt 1): 021302+, Aug. 2005.

Brilliantov, N. V. and T. Pöschel. Rolling friction of a viscous sphere on a hard plane. *EPL (Europhysics Letters)*, pages 511+, June 1998.

Brilliantov, N. V. and T. Pöschel. Granular Gases with impact-velocity dependent restitution coefficient. In Pöschel, T. and S. Luding, editors, *Granular Gases*, pages 101–124, Berlin, 2001. Springer.

Brilliantov, N. V. and T. Pöschel. *The Physics of Granular Media*, chapter Collision of Adhesive Viscoelastic Particles, pages 189–210. Wiley-VCH Verlag, June 6 2004.

Brilliantov, N. V. and T. Pöschel. *Kinetic Theory of Granular Gases*. Oxford University Press, Oxford, UK, 2004.

Brilliantov, N. V., F. Spahn, J. M. Hertzsch, and T. Pöschel. Model for collisions in granular gases. *Physical Review E*, 53(5):5382–5392, May 1996.

Brilliantov, N. V., T. Pöschel, and N. Brilliantov. *Kinetic Theory of Granular Gases*. Clarendon Press Oxford, 2003.

Brilliantov, N. V., T. Pöschel, W. T. Kranz, and A. Zippelius. Translations and Rotations Are Correlated in Granular Gases. *Physical Review Letters*, 98(12):128001+, Mar. 2007.

Carnahan, N. F. and K. E. Starling. Equation of state for nonattracting rigid spheres. *Journal of Chemical Physics*, 51:635, 1969.

Carnevale, G. F., Y. Pomeau, and W. R. Young. Statistics of ballistic agglomeration. *Physical Review Letters*, 64(24):2913–2916, June 1990.

Chernov, N. and R. Markarian. *Introduction to the ergodic theory of chaotic billiards*. IMPA Mathematical Publications]„ 2003.

Chokshi, A., A. G. G. M. Tielens, and D. Hollenbach. Dust coagulation. *Astrophys. J.*, 407:806–819, 1993.

Coppex, F., M. Droz, and E. Trizac. Hydrodynamics of probabilistic ballistic annihilation. *Physical Review E*, 70:061102+, Dec. 2004.

Dullweber, A., B. Leimkuhler, and R. McLachlan. Symplectic splitting methods for rigid body molecular dynamics. *The Journal of Chemical Physics*, 107(15):5840–5851, 1997.

Fiege, A., T. Aspelmeier, and A. Zippelius. Long-Time Tails and Cage Effect in Driven Granular Fluids. *Physical Review Letters*, 102:098001+, Mar. 2009.

Fingerle, A. *Entropy Production and Phase Transitions far from Equilibrium with Emphasis on Wet Granular Matter*. PhD thesis, University Göttingen, 2007.

Fingerle, A. and S. Herminghaus. Equation of state of wet granular matter. *Physical Review E (Statistical, Nonlinear, and Soft Matter Physics)*, 77(1):APS—21, 2007.

Fingerle, A., K. Roeller, K. Huang, and S. Herminghaus. Phase transitions far from equilibrium in wet granular matter. *New Journal of Physics*, 10(5):053020, 15 May 2008.

Fournier, Z., D. Geromichalos, S. Herminghaus, M. M. Kohonen, F. Mugele, M. Scheel, M. Schulz, B. Schulz, C. Schier, R. Seemann, and A. Skudelny. Mechanical properties of wet granular materials. *Journal of Physics: Condensed Matter*, 17(9):S477–S502, Mar. 2005.

Frenkel, D. and B. Smit. *Unterstanding Molecular Simulation - From Algorithms to Applications*. Academic Press, 2002.

Gaspard, P. *Chaos, Scattering and Statistical Mechanics*. Nonlinear Science Series. Cambridge University Press, 2005.

Gaspard, P. and J. R. Dorfman. Chaotic scattering theory, thermodynamic formalism, and transport coefficients. *Phys. Rev. E*, 52:3525–3552, Oct. 1995.

Glassmeier, F. *Ergodic Theory of Wet Granular Matter*. PhD thesis, University of Göttingen, 2010.

Gradshteyn, I. S. and I. M. Ryzhik. *Table of Integrals, Series, And Products*. Academic Press, 1980.

Hansen, J. and I. McDonald. *Theory of simple liquids*. Academic press, 2006.

Herminghaus, S. Dynamics of wet granular matter. *Advances In Physics*, 54(3):221–261, May 2005.

Hertz, H. Über die Berührung fester elastischer Körper. *J. Reine Angew. Math.*, 92: 156–171, 1882.

Hoover, W. G., C. G. Hoover, and M. N. Bannerman. Single-Speed Molecular Dynamics of Hard Parallel Squares and Cubes. *Journal of Statistical Physics*, 136(4):715–732, Aug. 2009.

Hornbaker, D. J., R. Albert, I. Albert, A.-L. Barabási, and P. Schiffer. What keeps sandcastles standing? *Nature*, 387:765, 19 June 1997.

Huang, K. *Statistical Mechanics*. Wiley, New York, 1987.

Iijima, S. Fine particles of silicon. I. Crystal growth of spherical particles of Si. *Jpn. J. Appl. Phys.*, 26, 1987.

Iverson, R. The physics of debris flows. *Review of Geophysics*, 35:245–296, 1997.

Khinchin, A. *Mathematical Foundations of Statistical Mechanics*. Dover Publications, 1949.

Kleider, M. Liquid-Gas Coexistence in Wet Granular Matter. Master's thesis, University Göttingen, 2012.

Landau, L. and E. Lifshitz. Elasticity theory. 1975.

Lees, A. W. and S. F. Edwards. The computer study of transport processes under extreme conditions. *Journal of Physics C: Solid State Physics*, 5(15):1921, 1972.

Liang, S. and L. P. Kadanoff. Scaling in a ballistic aggregation model. *Physical Review A*, 31:2628–2630, Apr. 1985.

Liao, C.-C. and S.-S. Hsiau. Experimental analysis of dynamic properties in wet sheared granular matter. *Powder Technology*, 197(3):222 – 229, 2010.

Lissauer, J. J. Planet Formation. *Annual Review of Astronomy and Astrophysics*, 31(1): 129–172, 1993.

Loskutov, A., O. Chichigina, and A. Ryabov. Thermodynamics of dispersing billiards with time-dependent boundaries. *Int. J. Bifurcat. Chaos*, 18:2863–2869, 2008.

Luding, S. *Die Physik trockener granularer Medien*. Logos Verlag, Berlin, 1998.

Luding, S. Towards dense, realistic granular media in 2D. *Nonlinearity*, 22:R101 – R146, 13 November 2009.

Lun, C. K. K., S. B. Savage, D. J. Jeffrey, and N. Chepurniy. Kinetic theories for granular flow: inelastic particles in Couette flow and slightly inelastic particles in a general flowfield. *Journal of Fluid Mechanics*, 140:223–256, 1984.

Mak, C. H. Large-scale simulations of the two-dimensional melting of hard disks. *Phys. Rev. E*, 73:065104, Jun 2006.

McLachlan, R. I. and P. Atela. The accuracy of symplectic integrators. *Nonlinearity*, 5(2): 541, 1992.

Mitarai, N. and F. Nori. Wet granular materials. *Advances in Physics*, 55(1-2):1–45, Jan 2006.

Montanero, J. M., V. Garz, A. Santos, and J. J. Brey. Kinetic theory of simple granular shear flows of smooth hard spheres. *Journal of Fluid Mechanics*, 389:391–411, 1999.

Müller, P. and T. Pöschel. Two-ball problem revisited: Limitations of event-driven modeling. *Physical Review E*, 83(4):041304+, Apr. 2011.

Nakagawa, M. and S. Luding, editors. *Powders and Grains 2009*. American Institute of Physics (AIP), Golden, Colorado, USA, 2009.

Nie, X., E. Ben-Naim, and S. Chen. Dynamics of freely cooling granular gases. *Physical Review Letters*, 89(20):204301, 2002.

Pearson, E. M., T. Halicioglu, and W. A. Tiller. Laplace-transform technique for deriving thermodynamic equations from the classical microcanonical ensemble. *Phys. Rev. A*, 32:3030–3039, Nov 1985.

Penrose, O. *Foundations of statistical mechanics*. Dover-Reprint, 2003.

Pöschel, T. and H. J. Herrmann. Size Segregation and Convection. *Europhysics Letters*, 29:123, 1995.

Pöschel, T. and T. Schwager. *Computational granular dynamics : models and algorithms*. Springer-Verlag, 2005.

Puglisi, A. Granular fluids, a short walkthrough. Dipartimento di Fisica, Universita La Sapienza, p.le Aldo Moro 2, 00181, Roma, Italy.

Radja, F. and S. Roux. *The Physics of Granular Media*, chapter Contact Dynamics Study of 2D Granular Media: Critical States and Relevant Internal Variables, pages 165–188. Wiley-VCH Verlag, June 6 2004.

Ramirez, R., T. Pöschel, N. V. Brilliantov, and T. Schwager. Coefficient of restitution of colliding viscoelastic spheres. *Phys. Rev. E*, 60:4465–4472, 1999.

Rapoport, A., V. Rom-Kedar, and D. Turaev. Stability in High Dimensional Steep Repelling Potentials. *Communications in Mathematical Physics*, 279(2):497–534, Apr. 2008.

Reichl, L. E. *A Modern Course in Statistical Physics*. Texas University Press, 1980.

Roeller, K. and S. Herminghaus. Solid-fluid transition and surface melting in wet granular matter. *EPL (Europhysics Letters)*, pages 26003+, Oct. 2011.

Röller, K. *Numerical simulations of wet granular matter*. PhD thesis, Georg-August-Universität Göttingen, 2010.

Scheel, M. *Experimental investigations of the mechanical properties of wet granular matter*. PhD thesis, Universität Göttingen, 2009.

Schwager, T. and T. Pöschel. Coefficient of Normal Restitution of Viscous Particles and Cooling Rate of Granular Gases. 1996.

Schäfer, J., S. Dippel, and D. E. Wolf. Force schemes in simulations of granular materials. *J. Physique I*, 6:5, 1996.

Shirts, R. B., S. R. Burt, and A. M. Johnson. Periodic boundary condition induced breakdown of the equipartition principle and other kinetic effects of finite sample size in classical hard-sphere molecular dynamics simulation. *The Journal of Chemical Physics*, 125, 2006.

Shokouhi, M. and G. A. Parsafar. The effect of steepness of soft-core square-well potential model on some fluid properties. *Molecular Physics*, 106(1):103–112, Jan. 2008.

Simányi, N. Proof of the Boltzmann-Sinai ergodic hypothesis for typical hard disk systems. *Inventiones Mathematicae*, 154(1):123–178, Oct. 2003.

Sinai, Y. G. On the foundations of the ergodic hypothesis for a dynamical system of statistical mechanics. *Doklady Akademii Nauk SSSR*, 153:1261–1264, 1963.

Sinai, Y. G. Dynamical systems with elastic reflections. *Russian Mathematical Surveys*, pages 137+, Oct. 2007.

Song, Y., E. Mason, and R. M. Stratt. Why does the Carnahan-Starling equation work so well? *Journal of Physical Chemistr*, 93:6916–6919, 1989.

Spahn, F., J. M. Hertzsch, and N. V. Brilliantov. The role of particle collisions for the dynamics in planetary rings. *Chaos, Solitons & Fractals*, 10:1945–1964, 1995.

Talu, I., G. I. Tardos, and M. I. Khan. Computer simulation of wet granulation. *Powder Technology*, 110(1-2):59 – 75, 2000.

Trizac, E. and J. P. Hansen. Dynamic Scaling Behavior of Ballistic Coalescence. *Physical Review Letters*, 74:4114–4117, May 1995.

Trizac, E. and P. L. Krapivsky. Correlations in Ballistic Processes. *Physical Review Letters*, 91:218302+, Nov. 2003.

Ulrich, S., T. Aspelmeier, K. Roeller, A. Fingerle, S. Herminghaus, and A. Zippelius. Cooling and Aggregation in Wet Granulates. *Physical Review Letters*, 102(14):148002+, Apr. 2009a.

Ulrich, S., T. Aspelmeier, A. Zippelius, K. Roeller, A. Fingerle, and S. Herminghaus. Dilute Wet Granulates: Nonequilibrium Dynamics and Structure Formation. *Physical Review E*, 80:031306, 2009b.

Vollmer, J. Chaos, spatial extension, transport, and non-equilibrium thermodynamics. *Physics Reports*, 372(2):131–267, 2002.

Wallis, M. K. Random fluctuations versus Poynting-Robertson drag on interplanetary dust grains. *Nature*, 320:146 – 148, 13 March 1986.

Walton, O. and R. Braun. Viscosity, granular temperature, and stress calculations for shearing assemblies of inelastic, frictional disks. *J. Rheol.*, 30:949, 1986.

Walton, O. R. Explicit particle dynamics model for granular materials. *Numerical Methods in Geosciences*, page 1261, 1982.

Willett, C. D., M. J. Adams, S. A. Johnson, and J. P. K. Seville. Capillary Bridges between Two Spherical Bodies. *Langmuir*, 16(24):9396–9405, 2000.

Yuste, S. B. and A. Santos. Sticky hard spheres beyond the Percus-Yevick approximation. *Physical Review E*, 48:4599–4604, Dec. 1993.

Zaburdaev, V. Y., M. Brinkmann, and S. Herminghaus. Free Cooling of the One-Dimensional Wet Granular Gas. *Physical Review Letters*, 97, 2006.

Zhu, H. P., Z. Y. Zhou, R. Yang, and A. B. Yu. Discrete particle simulation of particulate systems: Theoretical Developments. *Chemical Engineering Science*, 62:2278–3396, 2007.

Zippelius, A. Granular gases. *Physica A: Statistical Mechanics and its Applications*, 369 (1):143–158, Sept. 2006.

Erklärung

Nach §13(8) der Prüfungsordnung für den Bachelor-Studiengang Physik und den Master-Studiengang Physik an der Universität Göttingen: Hiermit erkläre ich, dass ich diese Abschlussarbeit selbständig verfasst habe, keine anderen als die angegebenen Quellen und Hilfsmittel benutzt habe und alle Stellen, die wörtlich oder sinngemäß aus veröffentlichten Schriften entnommen wurden, als solche kenntlich gemacht habe. Darüberhinaus erkläre ich, dass diese Abschlussarbeit nicht, auch nicht auszugsweise, im Rahmen einer nichtbestandenen Prüfung an dieser oder einer anderen Hochschule eingereicht wurde.

Göttingen, den 31. August 2012

Jan-Hendrik Trösemeier